AD-A168 749 IMPACT RESPONSE OF STRUCTURES--GLOBAL LOCAL APPROACH 1/1
(U) NORTHWESTERN UNIV EVANSTON IL L M KEER 01 DEC 84
AFOSR-TR-86-0287 AFOSR-82-0330

UNCLASSIFIED F/G 20/11 NL

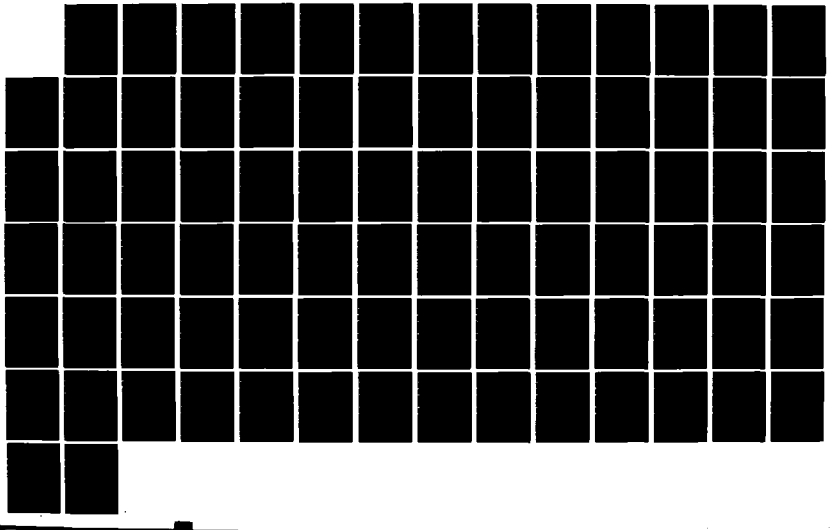

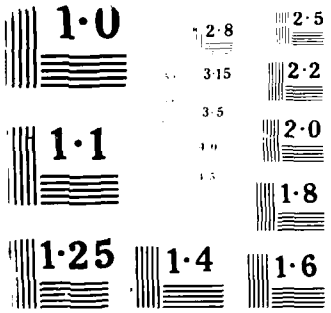
1·0
2·8
2·5
3·15
2·2
3·5
2·0
1·1
1·8
1·25
1·4
1·6

UNCLASSIFIED

(2)

REPORT DOCUMENTATION PAGE

AD-A168 749

1b. RESTRICTIVE MARKINGS

2b. DECLASSIFICATION/DOWNGRADING SCHEDULE

3. DISTRIBUTION/AVAILABILITY OF REPORT
Approved for public release; distribution unlimited.

4. PERFORMING ORGANIZATION REPORT NUMBER(S)

5. MONITORING ORGANIZATION REPORT NUMBER(S)
AFOSR [illegible]

6a. NAME OF PERFORMING ORGANIZATION: Northwestern University

6b. OFFICE SYMBOL (If applicable)

7a. NAME OF MONITORING ORGANIZATION: Air Force Office of Scientific Research/NA

6c. ADDRESS (City, State and ZIP Code)
Sponsored Projects Administration
619 Clark Street
Evanston, Illinois 60201

7b. ADDRESS (City, State and ZIP Code)
Bolling Air Force Base, D.C. 20332

8a. NAME OF FUNDING/SPONSORING ORGANIZATION: AFOSR

8b. OFFICE SYMBOL (If applicable): AFOSR/NA

9. PROCUREMENT INSTRUMENT IDENTIFICATION NUMBER: AFOSR-82-0330

8c. ADDRESS (City, State and ZIP Code)
AFOSR/NA
Building 410
Bolling AFB, D.C. 20332

10. SOURCE OF FUNDING NOS.

PROGRAM ELEMENT NO.	PROJECT NO.	TASK NO.	WORK UNIT NO.
61102F	2302	B1	

11. TITLE (Include Security Classification) IMPACT RESPONSE OF STRUCTURES--GLOBAL LOCAL APPROACH

12. PERSONAL AUTHOR(S) Leon M. Keer

13a. TYPE OF REPORT	13b. TIME COVERED	14. DATE OF REPORT (Yr., Mo., Day)	15. PAGE COUNT
Interim Report	FROM 10/1/83 TO 11/30/84	12/1/84	[illegible]

16. SUPPLEMENTARY NOTATION

17. COSATI CODES		
FIELD	GROUP	SUB. GR.

18. SUBJECT TERMS (Continue on reverse if necessary and identify by block number)
.Impact .Plates
.Indentation .Global-Local Analysis
.Beams .Elastic-Plastic Material

19. ABSTRACT (Continue on reverse if necessary and identify by block number)

Static and dynamic solutions to indentation problems of large area contact by a rigid indenter were solved. The major problems that were solved were the following:
1. LOW VELOCITY IMPACT ON A CIRCULAR PLATE by Keer and Woo. The problem of the dynamic impact of a rigid indenter striking a circular elastic plate was solved. The indenter was assumed to have a radius of curvature sufficiently large that areas of contact of the order of the plate thickness could be considered. Clamped and simply supported cases of impact were considered.
2. LOW VELOCITY IMPACT ON A TRANSVERSELY ISOTROPIC PLATE by Keer and Woo. The problem of the dynamic impact of a rigid indenter striking a transversely isotropic circular elastic plate was solved. The problem geometry and formulation was similar to (1) except that the material properties were for transverse isotropy. Three materials were chosen for this case: cadmium, magnesium, and a laminated composite.

(cont'd on reverse)

20. DISTRIBUTION/AVAILABILITY OF ABSTRACT
UNCLASSIFIED/UNLIMITED ☒ SAME AS RPT. ☐ DTIC USERS ☐

21. ABSTRACT SECURITY CLASSIFICATION
UNCLASSIFIED

22a. NAME OF RESPONSIBLE INDIVIDUAL

22b. TELEPHONE NUMBER (Include Area Code)

22c. OFFICE SYMBOL

DD FORM 1473, 83 APR — EDITION OF 1 JAN 73 IS OBSOLETE.

UNCLASSIFIED
SECURITY CLASSIFICATION OF THIS PAGE

ABSTRACT (cont'd)

3. SMOOTH INDENTATION OF AN ISOTROPIC CANTILEVER BEAM by Keer and Schonberg. The elastic response of a cantilever beam of finite length to a frictionless cylindrical and flat indenter is studied. Solutions are obtained through a global-local technique, which accounts for both the local behavior near the indenter, as well as the global beam behavior. Results are compared to Hertz theory and to beam theory solutions and comments on the validity of the linear elastic analysis are made.

4. SMOOTH INDENTATION OF A TRANSVERSELY ISOTROPIC CANTILEVER BEAM by Keer and Schonberg. The plane elastic response of a transversely isotropic beam of finite length to a frictionless cylindrical and flat indenter is studied. Local indenter stresses, as well as displacements and rotations are computed for each case and plotted for various ratios of contact width to beam length, and for various positions of the indenter. Each problem is solved using a nearly isotropic and a highly anisotropic material. Results are compared to those of the isotropic study, and to Hertz theory and beam theory solutions

RESEARCH OBJECTIVES

The objective of the research is to attempt to develop systematic techniques for determining the response to dynamic impact, when the shape of the impacting object is known. It is hoped that the dynamic response can be obtained by the use of techniques that accurately model the stresses near the point of impact as well as the stresses away from the point of impact. This technique is one that involves a global-local technique, where a more exact description of the stress distribution is made near the contact (for example, elasticity theory) and a more approximate theory is used away from the point of load application (beam, plate or shell theory). An analysis should incorporate the following features:

a. The elastic and/or plastic stresses in the vicinity of the impacting object must be accurately characterized.

b. An accurate description of the material must be used, especially when considering damage near the impact.

c. At points distant from the load the analysis must accurately model the dynamic response. Effects of support members, joints or other restraints on the response must be carefully modeled.

d. An evaluation of the potential towards damage, such as cracking, plastic deformation, delamination, etc. must be made.

The research objectives include the study of both static and dynamic solutions to indentation problems. The static ones are solved in order to understand the elasticity result that will tend to form the basis for the local solution. This solution will be incorporated into a dynamic structural mechanics solution for a beam, plate or shell to obtain results of both a global and local character. The first year of research concentrated on the solutions appropriate to beam theory and to axially symmetric plate theory.

STATUS OF THE RESEARCH

The research is progressing along the lines of the original proposal. The following are problems that involve the global-local approach that have been solved for the static case:

1. SMOOTH INDENTATION OF AN ISOTROPIC CANTILEVER BEAM by L.M. Keer and W. Schonberg. The elastic response of a cantilever beam of finite length to a frictionless cylindrical and flat indenter is studied. Solutions are obtained through a global-local technique, which accounts for both the local behavior near the indenter, as well as the global beam behavior. Results are compared to Hertz theory and to beam theory solutions and comments on the validity of the linear elastic analysis are made.

2. SMOOTH INDENTATION OF A TRANSVERSELY ISOTROPIC CANTILEVER BEAM by L.M. Keer and W. Schonberg. The plane elastic response of a transversely isotropic beam of finite length to a frictionless cylindrical and flat indenter is studied. Local indenter stresses, as well as displacements and rotations are computed for each case and plotted for various ratios of contact width to beam length, and for various positions of the indenter. Each problem is solved using a nearly isotropic and a highly anisotropic material. Results are compared to those of the isotropic study, and to Hertz theory and beam theory solutions.

An extension of these problems to the dynamic case is presently under way. Possible titles are given in "PAPERS IN PREPARATION"

The following are the dynamic problems that have been solved and are presently in press or being considered for publication.

1. LOW VELOCITY IMPACT ON A CIRCULAR PLATE by L.M. Keer and K.T. Woo. The problem of the dynamic impact of a rigid indenter striking a circular

elastic plate was solved. The indenter was assumed to have a radius of curvature sufficiently large that areas of contact of the order of the plate thickness could be considered. Clamped and simply supported cases of plate impact were considered.

2. LOW VELOCITY IMPACT ON A TRANSVERSELY ISOTROPIC PLATE by L.M. Keer and K.T. Woo. The problem of the dynamic impact of a rigid indenter striking a transversely isotropic circular elastic plate was solved. The problem geometry and formulation was similar to (1) except that the material properties were for transverse isotropy. Three materials were chosen for this case: cadmium, magnesium, and a laminated composite.

In addition to the above papers the dynamic impact of initially stressed beams and cantilever beams are papers in preparation. They should be submitted for publication relatively soon.

LIST OF WRITTEN PUBLICATIONS (DURATION OF GRANT)

1. L.M. Keer and G.R. Miller, "Smooth Indentation of Finite Layer", ASCE Journal of Engineering Mechanics, Vol. 109, 1983, pp. 706-717.
2. L.M. Keer and R. Ballarini, "Smooth Contact between a Rigid Indenter and an Initially Stressed Orthotropic Beam", AIAA Journal, Vol. 21, 1983 pp. 1035-1042.
3. L.M. Keer and J.C. Lee, "Dynamic Impact of an Elastically Supported Beam--Large Area Contact", International Journal of Engineering Science, in press.
4. L.M. Keer and W. Schonberg, "Smooth Indentation of an Isotropic Cantilever Beam", International Journal of Solids and Structures, in press. (Included with report).

LIST OF PAPERS PUBLISHED IN PROCEEDINGS

1. L.M. Keer and R. Ballarini, "Smooth Contact between a Rigid Indenter and Initially Stressed Orthotropic Beam", in Advances in Aerospace Structures, Materials and Dynamics, ASME (1982).
2. L.M. Keer and J.C. Lee, "Dynamic Impact of an Elastically Supported Beam--Large Area Contact", Advances in Aerospace Structures, Materials and Dynamics, ASME (1983).
3. L.M. Keer and K.T. Woo, "Low Velocity Impact on a Circular Plate" Advances in Aerospace Structures, Materials and Dynamics, ASME (1984) in press. (Included with report).

PAPERS SUBMITTED FOR PUBLICATION

1. L.M. Keer and W. Schonberg, "Smooth Indentation of a Transversely Isotropic Cantilever Beam".
2. L.M. Keer and K.T. Woo, "Low Velocity Impact on a Transversely Isotropic Plate".

PAPERS IN PREPARATION

1. L.M. Keer and W. Schonberg, "Dynamic Impact of an Elastically Supported Cantilever Beam".

2. L.M. Keer and W. Schonberg, "Dynamic Impact of an Initially Stressed, Orthotropic Beam".

PERSONNEL ASSOCIATED WITH RESEARCH EFFORT

1.	W. Schonberg	Research Assistant in Civil Engineering
2.	K.T. Woo	Research Assistant in Applied Mathematics (partially supported)
3.	J.C. Lee	Post Doctoral Fellow (partially supported)

SMOOTH INDENTATION OF AN ISOTROPIC CANTILEVER BEAM

by

Leon M. Keer and William P. Schonberg

Department of Civil Engineering

Northwestern University

Evanston, IL 60201

Abstract

The response of an isotropic cantilever beam of finite length under the action of frictionless cylindrical and flat indenters is studied. Solutions are obtained through a local-global technique, which accounts for both the local behavior near the indenter, as well as the global beam behavior. The method of analysis superposes an infinite layer solution derived through the use of integral transforms with a pure bending beam theory solution. Local indenter stresses, as well as displacements and rotations are computed for each case and plotted for various ratios of contact width to beam length, and for various positions of the indenter. Where possible, the results are compared to Hertz theory of contact stresses and to beam displacement and rotation solutions.

1. INTRODUCTION

Consider the finite layer of length ℓ and thickness h shown in Fig. 1. The layer is fixed at one end, free on the other, and loaded by an indenter centered at a distance ℓ_0 from the fixed end. Although the theory is applicable for an arbitrary geometry, the types of indenters studied are cylindrical (Fig. 1a) and flat (Fig. 1b). Such problems are seen quite often in mechanical applications and may also serve as models for impact phenomena in gears and turbine blades. Usual methods which use a beam theory solution to obtain an overall load-displacement relationship and then a Hertzian contact solution to calculate local stresses under the indenter are fairly limited, as will be shown in this paper. The method of solution used in this paper is the superposition of an elasticity solution with a beam theory solution. In this way, local contact stresses are represented by the elasticity solution, while the global stresses are represented by the beam theory solution.

A problem of the type considered here has already been solved by Keer and Miller [1], and by Keer and Ballarini [2] for a beam that is clamped or simply supported at both ends and loaded by a cylindrical indenter. Although not treated numerically here, the intermediate case of a partially fixed end can be solved for each type of indenter in a similar manner. Furthermore, the methods used in this paper can be modified and expanded to study plate or shell problems involving similar loadings [3].

The physical quantities of interest are the stress distribution under each indenter, and the displacement and rotation of the beam under each of the indenters. The ratio of contact width to beam thickness, c/h, is treated as a known parameter in both problems. In the cylindrical indenter problem, the

ratio of indenter arm length to beam thickness, ℓ_0/h, is treated as an additional known parameter. However, in the flat indenter problem, the parameter $\ell_1/h = \ell_0/h - c/h$ (i.e. the distance from the fixed end of the beam to the left-hand end of the indenter) is introduced as an additional known parameter. In this manner, for a given ℓ_1/h, when the quantity c/h is varied over a range of values the phenomenon known as "receding contact" can be observed in the flat indenter problem. By varying the proper parameters as required by the type of problem, then calculating deflections, rotations, loads and stresses, an extensive study of the response of an isotropic cantilever beam subjected to various loading conditions can be performed. The results obtained are compared to beam theory solutions and Hertz contact solutions for accuracy assessments.

2. CASE I: CYLINDRICAL INDENTER - PROBLEM FORMULATION

The problem to be solved is that of an elastic layer of thickness h and length ℓ indented by a cylindrical punch on its upper surface (Fig. 1a). The conditions at the ends of the layer are those of a cantilever beam, clamped on the left and free on the right. The solution of the problem will be achieved by a suitable superposition and matching of an elasticity solution and a beam theory solution.

The boundary conditions for the elasticity problem can be written as follows:

$$\tau_{yy}(x,h) = 0 \qquad |x| < \infty \qquad (2.1)$$

$$\tau_{xy}(x,h) = 0 \qquad |x| < \infty \qquad (2.2)$$

$$\tau_{xy}(x,0) = 0 \qquad |x| < \infty \qquad (2.3)$$

$$\tau_{yy}(x,0) = 0 \qquad c < |x| < \infty \qquad (2.4)$$

$$u_y(x,0) = \Delta - x^2/2R \qquad 0 < |x| < c. \qquad (2.5)$$

The beam theory boundary conditions for the ends of the layer can be written as follows:

$$\bar{\theta} = 0 \qquad x = -\ell_0 \qquad (2.6)$$

$$u_y = 0 \qquad x = -\ell_0 \qquad (2.7)$$

$$M = 0 \qquad x = \ell - \ell_0 \qquad (2.8)$$

$$V = 0 \qquad x = \ell - \ell_0 \qquad (2.9)$$

where M, V are the moment, shear and $\bar{\theta}$ is the average value of the slope measured through the thickness given by

$$\bar{\vartheta} = \frac{1}{h}\int_0^h \frac{\partial u_y}{\partial x}\, dy. \tag{2.10}$$

A suitable elasticity solution that represents loading on the upper surface of an isotropic elastic layer in plane strain with and no loading on its lower surface is obtained using the techniques of Sneddon [4] and is given as follows:

$$\tau_{yy} = \int_0^\infty \frac{E_S(\xi)\cos(\xi x)+E_A(\xi)\sin(\xi x)}{\beta^2-\sinh^2\beta} \{[\beta + \sinh\beta\cosh\beta + \xi y \sinh^2\beta]\sinh(\xi y)$$

$$- [\sinh^2\beta - \beta^2 + \xi y(\beta + \sinh\beta\cosh\beta)]\cosh(\xi y)\}d\xi \tag{2.11}$$

$$\tau_{xy} = -\int_0^\infty \frac{E_S(\xi)\sin(\xi x)-E_A(\xi)\cos(\xi x)}{\beta^2-\sinh^2\beta} \{[\beta^2 - \xi y(\beta + \sinh\beta\cosh\beta)]\sinh(\xi y)$$

$$+ \xi y \sinh^2\beta \cosh(\xi y)\}d\xi \tag{2.12}$$

$$\tau_{xx} = \int_0^\infty \frac{E_S(\xi)\cos(\xi x)+E_A(\xi)\sin(\xi x)}{\beta^2-\sinh^2\beta} \{[\beta + \sinh\beta - \xi y \sinh^2\beta]\sinh(\xi y)$$

$$- [\beta^2 + \sinh^2\beta - \xi y (\beta+\sinh\beta\cosh\beta)]\cosh(\xi y)\}d\xi \tag{2.13}$$

$$2\mu u_x = \int_0^\infty \frac{E_S(\xi)\sin(\xi x)-E_A(\xi)\cos(\xi x)}{\xi(\beta^2-\sinh^2\beta)} \{[(1-2\nu)(\beta + \sinh\beta\cosh\beta)- \xi y \sinh^2\beta]\sinh(\xi y)$$

$$- [\beta^2 + (1-2\nu)\sinh^2\beta - \xi y(\beta + \sinh\beta\cosh\beta)]\cosh(\xi y)\}d\xi \tag{2.14}$$

$$2\mu u_y = \int_0^\infty \frac{E_S(\xi)\cos(\xi x)+E_A(\xi)\sin(\xi x)}{\xi(\beta^2-\sinh^2\beta)} \{[\beta^2 - 2(1-\nu)\sinh^2\beta - \xi y(\beta + \sinh\beta\cosh\beta)]\sinh(\xi y)$$

$$+ [2(1-\nu)(\beta + \sinh\beta\cosh\beta) + \xi y \sinh^2\beta]\cosh(\xi y)\}d\xi. \tag{2.15}$$

where $\beta = \xi h$, and u, ν are the shear modulus and Poisson's Ratio of the layer material, respectively. The corresponding equations for a layer in plane stress with the same loading conditions are obtained by replacing ν with $\nu/(1+\nu)$. Furthermore, this substitution is to be used through the rest of this paper to convert plane strain expressions to corresponding expressions in plane stress.

It is seen that on $y = h$ the normal and shear stresses vanish automatically, and that on $y = 0$, the shear stresses vanish. The normal stress on $y = 0$ is given as

$$\tau_{yy}(x,0) = \int_0^\infty [E_S(\xi)\cos(\xi x) + E_A(\xi)\sin(\xi x)]d\xi. \tag{2.16}$$

We let

$$E_S(\xi) = \int_0^c \psi(t)J_0(\xi t)dt \tag{2.17}$$

$$E_A(\xi) = \int_0^c \phi(t)J_1(\xi t)dt. \tag{2.18}$$

Then Eqn. (2.16) becomes

$$\tau_{yy}(x,0) = \int_x^c \frac{\psi(t)dt}{\sqrt{t^2 - x^2}} + x \int_x^c \frac{\phi(t)dt}{t\sqrt{t^2 - x^2}}. \tag{2.19}$$

The moment and shear due to the stresses as given by Eqns. (2.11)-(2.13) are given by

$$M_E(x) = \int_0^h y\tau_{xx}dy = -\int_0^\infty [E_S(\xi)\cos(\xi x)+E_A(\xi)\sin(\xi x)]\frac{d\xi}{\xi^2} \tag{2.20}$$

$$V_E(x) = \int_0^h \tau_{xy} dy = \int_0^\infty [E_S(\xi)\sin(\xi x) - E_A(\xi)\cos(\xi x)] \frac{d\xi}{\xi} . \qquad (2.21)$$

We note that Eqns. (2.20), (2.21) satisfy the condition

$$V = \frac{dM}{dx} . \qquad (2.22)$$

From Eqns. (2.10), (2.15) the average value of the slope is found to be given by

$$\bar{\theta}_E(x) = \frac{1}{2\mu} \int_0^\infty \frac{\beta-(3-2\nu)\sinh\beta}{\beta(\beta-\sinh\beta)} [E_S(\xi)\sin(\xi x) - E_A(\xi)\cos(\xi x)] d\xi. \qquad (2.23)$$

For the beam theory solution, the displacement is taken to be of the form

$$u_y^B(x) = a_0 + a_1 x + a_2 x^2 + a_3 x^3. \qquad (2.24)$$

Assuming the hypotheses of Euler-Bernoulli Beam Theory, the following results are obtained:

$$u_x^B(x) = -\frac{\partial u_y^B}{\partial x}(y - \frac{h}{2}) \qquad (2.25)$$

$$\tau_{xx}^B = \frac{2\mu}{1-\nu} \frac{\partial u_x^B}{\partial x} \qquad (2.26)$$

Using Eqns. (2.24)-(2.26), the moment, shear and average slope are calculated to be,

$$M_B(x) = \int_0^h y\tau_{xx} dx = -2D(a_2 + 3a_3 x) \qquad (2.27)$$

$$V_B(x) = \int_0^h \tau_{xy} dx = -6Da_3 \tag{2.28}$$

$$\bar{\vartheta}_B(x) = \frac{1}{h}\int_0^h \frac{\partial u_x^B}{\partial x} dy = a_1 + 2a_2 x + 3a_3 x^2 \tag{2.29}$$

where $D = \mu h^3/6(1-\nu)$. Thus, the solution sought will be a superposition of the elasticity solution given by Eqns. (2.11)-(2.16), (2.20)-(2.23) and the beam theory solution given by Eqns. (2.24)-(2.29). The two solutions are matched properly when the boundary conditions, Eqns. (2.1)-(2.9) are all satisfied. This is achieved by solving for the constants a_1, a_2 and a_3 by superposing the two solutions and applying the beam theory boundary conditions. Thus, Eqns. (2.6), (2.8) and (2.9) become

$$M_E(\ell-\ell_0) + M_B(\ell-\ell_0) = 0 \tag{2.30}$$

$$V_E(\ell-\ell_0) + V_B(\ell-\ell_0) = 0 \tag{2.31}$$

$$\bar{\vartheta}_E(-\ell_0) + \bar{\vartheta}_B(-\ell_0) = 0. \tag{2.32}$$

Applying Eqns. (2.20)-(2.23) and (2.24)-(2.29) to Eqns. (2.30)-(2.32) yields the following:

$$a_1 = -\frac{1}{D}\int_0^\infty \left\{\frac{\ell_0(\ell-\ell_0/2)}{\xi}\left[E_S(\xi)\sin\xi(\ell-\ell_0) - E_A(\xi)\cos\xi(\ell-\ell_0)\right]\right.$$

$$\left. + \frac{\ell_0}{\xi^2}\left[E_S(\xi)\cos\xi(\ell-\ell_0) + E_A(\xi)\sin\xi(\ell-\ell_0)\right]\right\} d\xi$$

$$+ \frac{1}{2\mu}\int_0^\infty \frac{\beta-(3-2\nu)\sinh\beta}{\beta(\beta-\sinh\beta)}\left[E_S(\xi)\sin(\xi\ell_0) + E_A(\xi)\cos(\xi\ell_0)\right] d\xi \tag{2.33}$$

$$a_2 = -\frac{1}{D}\int_0^\infty \left[E_S(\xi)\cos\xi(\ell-\ell_0) + E_A(\xi)\sin\xi(\ell-\ell_0)\right]\frac{d\xi}{\xi^2}$$

$$- \frac{\ell-\ell_0}{2D} \int_0^\infty [E_S(\xi)\sin\xi(\ell-\ell_0) - E_A(\xi)\cos\xi(\ell-\ell_0)] \frac{d\xi}{\xi} \tag{2.34}$$

$$a_3 = \frac{1}{6D} \int_0^\infty [E_S(\xi)\sin\xi(\ell-\ell_0) - E_A(\xi)\cos\xi(\ell-\ell_0)] \frac{d\xi}{\xi} . \tag{2.35}$$

The two remaining boundary conditions given by Eqns. (2.5) and (2.7) still need to be satisfied. First, consider Eqn. (2.5):

$$u_y^E(x,0) + u_y^B(x,0) = \Delta - x^2/2R \tag{2.36}$$

Differentiating with respect to x:

$$\frac{\partial u_y^E}{\partial x}(x,0) + \frac{\partial u_y^B}{\partial x}(x,0) = - \frac{x}{R} . \tag{2.37}$$

Separating Eqn. (2.37) into a symmetric and an antisymmetric part with respect to x yields

$$\frac{\partial u_y^E}{\partial x}(x,0)\Big|_A + 2a_2x = - \frac{x}{R} \tag{2.38}$$

$$\frac{\partial u_y^E}{\partial x}(x,0)\Big|_S + a_1 + 3a_3x^2 = 0. \tag{2.39}$$

Consider first Eqn. (2.38). Substituting for $u_y^E(x,0)$ according to Eqn. (2.15), combining terms in $E_S(\xi)$ and $E_A(\xi)$, and making use of Eqns. (2.17), (2.18) yields

$$\int_0^c \psi(t) \int_0^\infty [\frac{h^3}{D}(\frac{\beta+sh\beta ch\beta}{\beta^2-sh^2\beta})\sin(\xi x) + \frac{x}{\xi^2}\cos\xi(\ell-\ell_0) + \frac{x(\ell-\ell_0)}{\xi}\sin\xi(\ell-\ell_0)]J_0(\xi t)d\xi dt$$

$$- \int_0^c p(t) \int_0^\infty [\frac{x}{\xi^2}\sin\xi(\ell-\ell_0) - \frac{x(\ell-\ell_0)}{\xi}\cos\xi(\ell-\ell_0)]J_1(\xi t)d\xi dt = \frac{\partial x}{\partial t} \tag{2.40}$$

An asymptotic evaluation of the kernels in Eqn. (2.40) shows that they are all convergent at the lower limit of integration. However, at the upper limit the first term in the first kernel is divergent. This is adjusted by adding and subtracting the term

$$\frac{h^3}{6}\int_0^c \psi(t)\int_0^\infty \sin(\xi x)J_0(\xi t)d\xi dt$$

in Eqn. (2.40) as follows:

$$-\frac{h^3}{6}\int_0^c \psi(t)\int_0^\infty \sin(\xi x)J_0(\xi t)d\xi dt + \int_0^c \psi(t)\int_0^\infty \left[\frac{h^3}{6}\left(\frac{\beta+sh\beta ch\beta}{\beta^2-sh^2\beta}+1\right)\sin(\xi x)\right.$$

$$\left.+\frac{x}{\xi^2}\cos\xi(\ell-\ell_0)+\frac{x(\ell-\ell_0)}{\xi}\sin\xi(\ell-\ell_0)\right]J_0(\xi t)d\xi dt$$

$$+\int_0^c \phi(t)\int_0^\infty \left[\frac{x}{\xi^2}\sin\xi(\ell-\ell_0)-\frac{x(\ell-\ell_0)}{\xi}\cos\xi(\ell-\ell_0)\right]J_1(\xi t)d\xi dt = \frac{Dx}{R} \quad (2.41)$$

After simplification (i.e. through use of the Weber-Schafheitlin Integral [5]), Eqn. (41) reduces to

$$\frac{h^3}{6}\psi(x)-\int_0^c \psi(t)K_1(x,t)dt-\int_0^c \phi(t)K_2(x,t)dt = -\frac{Dx}{R} \quad (2.42)$$

where

$$K_1(x,t) = \int_0^\infty \left[\frac{h^3}{6}\left(\frac{\beta+sh\beta ch\beta}{\beta^2-sh^2\beta}+1\right)\xi x J_0(\xi x)+\frac{x}{\xi^2}\cos\xi(\ell-\ell_0)\right]J_0(\xi t)d\xi + \frac{\pi}{2}x(\ell-\ell_0) \quad (2.43)$$

$$K_2(x,t) = \frac{\pi}{\ell}tx. \quad (2.44)$$

Returning to Eqn. (2.39), performing similar manipulations yields

$$\int_0^c \phi(t) \int_0^\infty \{\frac{h^3}{6} \frac{\beta+sh\beta ch\beta}{\beta^2-sh^2\beta} \cos(\xi x) + \frac{h^3}{12(1-\nu)} \frac{\beta-(3-2\nu)sh\beta}{\beta(\beta-sh\beta)} \cos(\xi \ell_0)$$

$$+ \frac{\ell_0(\ell-\ell_0/2)}{\xi} \cos\xi(\ell-\ell_0) - \frac{\ell_0}{\xi^2} \sin\xi(\ell-\ell_0) - \frac{x^2}{2\xi}\cos\xi(\ell-\ell_0)\}J_0(\xi t)d\xi dt$$

$$+ \int_0^c \psi(t) \int_0^\infty \{\frac{h^3}{12(1-\nu)} \frac{\beta-(3-2\nu)sh\beta}{\beta(\beta-sh\beta)} \sin(\xi \ell_0) - \frac{\ell_0(\ell-\ell_0/2)}{\xi} \sin\xi(\ell-\ell_0)$$

$$+ \frac{x^2}{2\xi} \sin\xi(\ell-\ell_0) - \frac{\ell_0}{\xi^2} \cos\xi(\ell-\ell_0)\}J_0(\xi t)d\xi dt = 0. \qquad (2.45)$$

An asymptotic analysis reveals that all the terms are bounded as $\xi \to 0$, but as $\xi \to \infty$ the first term of the first kernel is divergent. This is corrected by adding and subtracting the term

$$\frac{h^3}{6} \int_0^c \phi(t) \int_0^\infty \cos(\xi x)J_1(\xi t)d\xi dt$$

in Eqn. (2.45) as follows:

$$- \frac{h^3}{6} \int_0^c \phi(t) \int_0^\infty \cos(\xi x)J_1(\xi t)d\xi dt + \int_0^c \phi(t) \int_0^\infty \{\frac{h^3}{6} (\frac{\beta+sh\beta ch\beta}{\beta^2-sh^2\beta} + 1)\cos(\xi x)$$

$$+ \frac{h^3}{12(1-\nu)} \frac{\beta-(3-2\nu)sh\beta}{\beta(\beta-sh\beta)} \cos(\xi \ell_0) + \frac{\ell_0(\ell-\ell_0/2)}{\xi} \cos\xi(\ell-\ell_0)$$

$$- \frac{\ell_0}{\xi^2} \sin\xi(\ell-\ell_0) - \frac{x^2}{2\xi} \cos\xi(\ell-\ell_0)\}J_1(\xi t)d\xi dt$$

$$+ \int_0^c \psi(t) \int_0^\infty \{\frac{h^3}{12(1-\nu)}(\frac{\beta-(3-2\nu)sh\beta}{\beta(\beta-sh\beta)})\sin(\xi \ell_0) - \frac{\ell_0(\ell-\ell_0/2)}{\xi} \sin\xi(\ell-\ell_0)$$

$$- \frac{\ell_0}{\xi^2} \cos\xi(\ell-\ell_0) + \frac{x^2}{2\xi} \sin\xi(\ell-\ell_0)\}J_0(\xi t)d\xi dt = 0. \qquad (2.46)$$

After simplification Eqn. (2.46) becomes

$$\frac{h^3}{6}\phi(x) + \int_0^c \psi(t)K_3(x,t)dt - \int_0^c \phi(t)K_4(x,t)dt = 0 \qquad (2.47)$$

where

$$K_3(x,t) = \frac{\pi}{4}x^2 \qquad (2.48)$$

$$K_4(x,t) = \int_0^\infty \frac{h^3}{6}\left(\frac{\beta+sh\beta ch\beta}{\beta^2-sh^2\beta} + 1\right)\xi x J_1(\xi x)J_1(\xi t)d\xi. \qquad (2.49)$$

Eqns. (2.42) and (2.47) are the two coupled integral equations for the unknown auxiliary functions $\psi(x)$, $\phi(x)$. These equations are solved numerically. Once $\psi(x)$, $\phi(x)$ are obtained, all necessary physical quantities may be calculated.

Stresses may be calculated using Eqn. (2.19):

$$\tau_{yy}(x,0) = \int_x^c \frac{\psi(t)dt}{\sqrt{t^2-x^2}} + x\int_x^c \frac{\phi(t)\,dt}{t\sqrt{t^2-x^2}}. \qquad (2.19)$$

The resultant load due to the symmetric stresses is obtained as follows:

$$P = -\int_{-c}^{c} \tau_{yy}dx = -\pi\int_0^c \psi(t)dt. \qquad (2.50)$$

The resultant moment due to the antisymmetric stresses is obtained as follows:

$$M = -\int_{-c}^{c} x\tau_{yy}dx = -\frac{\pi}{2}\int_0^c t\phi(t)dt. \qquad (2.51)$$

In order to evaluate the deflection under the indenter, Δ, the constant a_0 must be determined. Superimposing Eqns. (2.15) and (2.24) yields

$$u_y(x,0) = \frac{1-\nu}{\mu} \int_0^\infty \frac{\beta + sh\beta ch\beta}{\xi(\beta^2-sh^2\beta)} [E_S(\xi)cos(\xi x) + E_A(\xi)sin(\xi x)]d\xi$$

$$+ a_0 + a_1 x + a_2 x^2 + a_3 x^3. \qquad (2.52)$$

Applying Eqn. (2.7) yields

$$a_0 = -(\frac{1-\nu}{\mu}) \int_0^\infty \frac{\beta+sh\beta ch\beta}{\beta^2-sh^2\beta} [E_S(\xi)cos(\xi\ell_0) - E_A(\xi)sin(\xi\ell_0)]\frac{d\xi}{\xi} + a_1\ell_0 - a_2\ell_0^2 + a_3\ell_0^3 \qquad (2.53)$$

where a_1, a_2, a_3 are given by Eqns. (2.33)-(2.35). Substituting Eqns. (2.33)-(2.35), (2.53) into Eqn. (2.52) and recalling that $u_y(0,0) = \Delta$ yields

$$\Delta = \int_0^c \psi(t)[\int_0^\infty \{\frac{1-\nu}{\mu} \frac{\beta+sh\beta ch\beta}{\beta^2-sh^2\beta}(\frac{1-cos\xi\ell_0}{\xi}) + \frac{\ell_0}{2\mu} \frac{\beta-(3-2\nu)sh\beta}{\beta(\beta-sh\beta)} sin(\xi\ell_0)$$

$$- \frac{\ell_0^2}{2D} \frac{cos\xi(\ell-\ell_0)}{\xi^2}\} J_0(\xi t)d\xi - \frac{\pi}{12D} \ell_0^2(3\ell-\ell_0)]dt$$

$$+ \int_0^c \phi(t)[\int_0^\infty \{\frac{1-\nu}{\mu} \frac{\beta+sh\beta ch\beta}{\beta^2-sh^2\beta} \frac{sin\xi\ell_0}{\xi} + \frac{\ell_0}{2\mu} \frac{\beta-(3-2\nu)sh\beta}{\beta(\beta-sh\beta)} cos(\xi\ell_0)\}J_1(\xi t)d\xi$$

$$- \frac{\pi t}{8D} \ell_0^2]dt. \qquad (2.54)$$

An asymptotic analysis reveals that both kernels are bounded as $\xi \to 0$, but the first two terms in each kernel are divergent as $\xi \to \infty$. This is adjusted by adding and subtracting the appropriate terms to yield

$$\Delta = \int_0^c \psi(t)K_5(t)dt + \int_0^c \phi(t)K_6(t)dt \qquad (2.55)$$

where

$$K_5(t) = \frac{1-\nu}{\mu}\int_0^\infty \{\left(\frac{\beta+sh\beta ch\beta}{\beta^2-sh\beta^2}+1\right)\left(\frac{1-\cos\xi\ell_0}{\xi}\right) - \frac{\ell_0}{h}\frac{\sin(\xi\ell_0)}{\beta - sh\beta}$$

$$- \frac{3\ell_0^2}{h^3}\frac{\cos\xi(\ell-\ell_0)}{\xi^2}\}J_0(\xi t)d\xi - \frac{1-\nu}{\mu}\cosh^{-1}\left(\frac{\ell_0}{t}\right)$$

$$+ \frac{\pi}{4}\frac{3-2\nu}{\mu h}\ell_0 - \frac{\pi}{12D}\ell_0^2(3\ell-\ell_0) \qquad (2.56)$$

$$K_6(t) = \frac{1-\nu}{\mu}\int_0^\infty \left(\frac{\beta+sh\beta ch\beta}{\beta^2-sh^2\beta}+1\right)\frac{\sin(\xi\ell_0)}{\xi} - \frac{\ell_0}{h}\frac{\cos(\xi\ell_0)}{\beta - sh\beta}\}J_1(\xi t)d\xi$$

$$- \frac{1-\nu}{\mu}\frac{t}{\ell_0+\sqrt{\ell_0^2-t^2}} - \frac{\pi t}{8D}\ell_0^2. \qquad (2.57)$$

A quantity of interest in this problem, as well as in the subsequent study of the dynamic case, is the rotation of the beam under the indenter. More specifically, the rotation of the beam at the point under the indenter about which the moment produced by the antisymmetric stresses is zero (i.e. the "eccentricity" of the load) is of special interest. This point is obtained from statics simply as

$$x = -e = M/P. \qquad (2.58)$$

Superimposing Eqns. (2.23) and (2.29) and making use of Eqns. (2.17), (2.18) and (2.33)-(2.35) yields

$$\bar{\theta}(x) = \frac{1}{D}\int_0^c \psi(t)\int_0^\infty \{\frac{h^3}{12(1-\nu)}\frac{\beta-(3-2\nu)sh\beta}{\beta(\beta-sh\beta)}(\sin\xi x+\sin\xi\ell_0)$$

$$-[\ell_0(\ell-\ell_0/2)+x(\ell-\ell_0)-x^2/2]\frac{\sin\xi(\ell-\ell_0)}{\xi} - (\ell_0+x)\frac{\cos\xi(\ell-\ell_0)}{\xi^2}\}J_0(\xi t)d\xi dt$$

$$+\frac{1}{D}\int_0^c \phi(t)\int_0^\infty \{-\frac{h^3}{12(1-\nu)}\frac{\beta-(3-2\nu)\sinh\beta}{\beta(\beta-\sinh\beta)}(\cos\xi x-\cos\xi\ell_0)$$

$$+[\ell_0(\ell-\ell_0/2)+x(\ell-\ell_0)-x^2/2]\frac{\cos\xi(\ell-\ell_0)}{\xi}-(\ell_0+x)\frac{\sin\xi(\ell-\ell_0)}{\xi^2}\}J_1(\xi t)d\xi dt. \tag{2.59}$$

Note that the boundary condition $\bar{\theta}(-\ell_0) = 0$ is automatically satisfied by Eqn. (2.59). An asymptotic analysis of the kernels in Eqn. (2.59) reveals that they are bounded as $\xi \to 0$, but that as $\xi \to \infty$, the first term in each is divergent. This can be adjusted as before to become the following:

$$\bar{\theta}(x) = \frac{1}{D}\int_0^c \psi(t)\{\int_0^\infty [-\frac{h^3}{6}(\frac{\sin\xi x+\sin\xi\ell_0}{\beta-\sinh\beta})-(x+\ell_0)\frac{\cos\xi(\ell-\ell_0)}{\xi^2}]J_0(\xi t)d\xi$$

$$-\frac{\pi}{2}[\ell_0(\ell-\ell_0/2)+x(\ell-\ell_0)-x^2/2]+\frac{\pi h^2}{24}\frac{3-2\nu}{1-\nu}\}dt$$

$$+\frac{1}{D}\int_0^c \phi(t)\{\int_0^\infty [\frac{h^3}{6}(\frac{\cos\xi x-\cos\xi\ell_0}{\beta-\sinh\beta})J_1(\xi t)]d\xi-\frac{\pi}{4}(\ell_0+x)\}dt$$

$$+\operatorname{sgn}(x)\left(\frac{3-2\nu}{2\mu h}\right)[\frac{\pi}{2}\int_0^{|x|}\psi(t)dt+\int_{|x|}^c \psi(t)\sin^{-1}(\frac{|x|}{t})dt]H(c-|x|)$$

$$-\frac{3-2\nu}{2\mu h}H(c-|x|)\int_{|x|}^c \frac{\phi(t)}{t}\sqrt{t^2-x^2}\,dt. \tag{2.60}$$

Thus, we can easily evaluate $\bar{\theta}$ $(x = -e)$.

3. PROBLEM SOLUTION

In order to be able to solve for the auxiliary functions $\psi(x)$, $\phi(x)$, Eqns. (2.42)-(2.44), (2.47)-(2.48) must be non-dimensionalized. This is

accomplished by the use of the following non-dimensional parameters:

$$\delta = c/h \qquad \varepsilon = e/h \qquad \psi(x) = \frac{Dcy}{Rh^3}\Psi(y) \qquad (3.1a,b),\ (3.2)$$

$$\alpha = \ell_0/h \qquad \gamma = \ell/h \qquad \phi(x) = \frac{Dcy}{Rh^3}\Phi(y). \qquad (3.1c,d),\ (3.3)$$

$$u = t/c \qquad y = x/c \qquad (3.1e,f)$$

Once the non-dimensionalized auxiliary functions $\Psi(y)$, $\Phi(y)$ are obtained, Eqns. (2.19), (2.50), (2.51), (2.55)-(2.57) and (2.60) can be used to calculate non-dimensionalized stresses, loads, moments, deflections and rotations, respectively. These non-dimensional quantities may be transformed back to real quantities via the following relationships:

$$\tau_{yy} = P\,\hat{\tau}_{yy}/c \qquad \Delta = h^2\hat{\Delta}/R \qquad (3.4),\ (3.7)$$

$$P = h^2\mu\hat{P}/(1-\nu)R \qquad \bar{\theta} = h\,\hat{\bar{\theta}}/R. \qquad (3.5),\ (3.8)$$

$$M = h^3\mu\hat{M}/(1-\nu)R \qquad (3.6)$$

In order to assess the accuracy of the results for displacement and rotation under the indenter, the following beam theory solutions are used:

$$\Delta_B = \frac{1}{3D}P\ell_0^3 + \frac{1}{2D}M\ell_0^2 \qquad (3.9)$$

$$\bar{\theta}_B = \frac{1}{2D}P(\ell_0^2-e^2) + \frac{1}{D}M(\ell_0-e) \qquad (3.10)$$

It should be noted that, although the formulation of the equations in this paper is such that they can be adapted to plane stress or plane strain,

the use of beam theory equations in comparison studies dictates that conditions of plane stress should be assumed in the evaluation of Eqns. (2.55) and (2.60). This assumption would be consistent with the use of a thin beam in an experimental verification of the results presented here. For the numerical evaluation of Eqns. (2.55) and (2.60) under conditions of plane stress, Poisson's Ratio is taken to be equal to 0.35 (this corresponds to a Poisson's Ratio of 0.26 if Eqns (2.55), (2.60) were to be evaluated under conditions of plane strain).

4. OBSERVATIONS AND CONCULSIONS

Solutions to the problem were obtained for δ = 0.2, 0.5 and 1.0, γ = 5.0, 10.0, 15.0 and 20.0, and for each γ, $\alpha = 0.25\gamma$, 0.5γ, 0.75γ. It was found that the stress distributions for the different values of ℓ/h remained virtually identical. This is illustrated in Tables 1 and 2, which compare peak symmetric and total stresses for different values of c/h and ℓ_0/h. A typical symmetric stress distribution is shown in Fig. 2; that of the total stress under the indenter is shown in Fig. 3. As can be seen in Fig. 2, for small values of c/h the Hertzian distribution approximates the stress under the indenter quite well. As c/h increases, the distribution changes significantly. In Fig. 3 we see that as c/h increases, the location of peak stress shifts to the left and the distribution becomes less and less parabolic. This is because for small values of c/h, the indenter acts like a point load. Hence, for small c/h, we have a small region of concentrated stress. However, as c/h increases, the shape of the indenter becomes more and more significant. As such, the curvature of the beam is much more pronounced, and the location of peak stress shifts to the left of the origin.

Tables 3 and 4 show a comparison between the elasticity solution developed here and the classical beam theory solution. The elasticity solution is seen to agree well with the beam theory solution. However, as c/h approaches ℓ_0/h the two solutions differ to a much larger extent. This behavior is due to the fact that the elasticity solution is valid only for $c/h \ll \ell_0/h$.

It is important to note that the rotations in Table 4 have no meaning unless they are converted to real values. Since the elasticity and beam theory solutions were derived using small angle approximations, it must be ensured that $\hat{\theta} < \theta_0$, where θ_0 is a predetermined angle below which rotations are considered "small." Thus, it is possible to place a lower bound on R, the radius of curvature of the indenter:

$$R/h > \hat{\theta}/\theta_0. \tag{4.1}$$

However, it must also be ensured that no yielding occurs anywhere in the beam, i.e., that $\sigma_{max} < \sigma_y$, where

$$\sigma_{max} = M_{max} h/2I_0, \qquad I_0 = h^3/12 \tag{4.2), (4.3}$$

and σ_y is the yield stress of the material. The maximum moment occurs at the fixed end of the beam and is given by

$$M_{max} = P\ell_0 - M. \tag{4.4}$$

This condition on σ_{max} yields another lower bound on R:

$$R/h > 6\mu(\alpha\hat{P}-\hat{M})/(1-\nu)\sigma_y \qquad (4.5)$$

If $\bar{\vartheta}_0 = 20^0$ (0.349 rad), $\sigma_y = 55{,}000$ ksi and $\mu = 11{,}510$ ksi, then Eqns. (4.1) and (4.5) may be combined into the following:

$$R/h > \max\{2.865\hat{\vartheta},\ 1.696(\alpha\hat{P}-\hat{M})\}. \qquad (4.6)$$

Judging from the values of $\hat{\vartheta}$, $\hat{P}$ and $\hat{M}$, it is evident that $2.865\hat{\vartheta} >> 1.696(\alpha\hat{P} - \hat{M})$ for each case considered. Thus, Eqn. (4.6) reduces to

$$R/h > 2.865\hat{\vartheta}. \qquad (4.7)$$

Under these criteria, Table 5 shows the minimum allowable values of R/h to ensure small deflections and no yielding. It is seen that for large c/h and for long beams with c/h > 0.5, the indenter is practically flat. It is, therefore, of some interest to solve the problem of a flat indenter. This solution is found in the next section.

6. CASE II: FLAT INDENTER - PROBLEM FORMULATION

The problem to be solved is that of an elastic layer of thickness h and length ℓ indented by a flat punch on its upper surface (Fig. 1b). The boundary conditions for the elasticity problem and beam theory problem whose solutions shall be superposed to form the solution to the actual problem are as follows:

$$\tau_{yy}(x,h) = 0 \qquad |x| < \infty \tag{5.1}$$

$$\tau_{xy}(x,h) = 0 \qquad |x| < \infty \tag{5.2}$$

$$\tau_{xy}(x,0) = 0 \qquad |x| < \infty \tag{5.3}$$

$$\tau_{yy}(x,0) = 0 \qquad c < |x| < \infty \tag{5.4}$$

$$u_y(x,0) = \Delta \qquad 0 < |x| < c \tag{5.5}$$

$$\bar{\theta} = 0 \qquad x = -\ell_0 \tag{5.6}$$

$$u_y = 0 \qquad x = -\ell_0 \tag{5.7}$$

$$M = 0 \qquad x = \ell - \ell_0 \tag{5.8}$$

$$V = 0 \qquad x = \ell - \ell_0 \tag{5.9}$$

It is further imposed that the stresses be non-singular at $x = c$:

$$|\tau_{yy}(c,0)| < \infty. \tag{5.10}$$

This condition ensures a smooth deflection of the beam for $x > 0$ and results in a "receding contact" [6]; here, as the load, increases, the contact length decreases with load.

Ths suitable elasticity solution for this problem is given by Eqns. (2.11) through (2.15). Using this formulation, the normal stress is given by

$$\tau_{yy}(x,0) = \int_0^\infty [E_S(\xi)\cos\xi x + E_A(\xi)\sin\xi x]d\xi. \tag{5.11}$$

For a flat punch, to have singularities at $x = \pm c$, we let

$$E_S'(\xi) = AJ_0(\xi c) + \int_0^c \psi(t)J_0(\xi t)dt \tag{5.12}$$

$$E_A(\xi) = BJ_1(\xi c) + \int_0^c \phi(t)J_1(\xi t)d\xi. \tag{5.13}$$

Substituting into Eqn. (5.11) yields

$$\tau_{yy}(x,0) = \frac{A + \frac{x}{c}B}{\sqrt{c^2-x^2}} H(c-x) + \int_x^c \frac{\psi(t)dt}{\sqrt{t^2-x^2}} + x\int_x^c \frac{\phi(t)dt}{t\sqrt{t^2-x^2}}. \tag{5.14}$$

The first term in Eqn. (5.14) is singular at $x = \pm c$. For the singularity to vanish at $x = c$, it must be true that $A + B = 0$. Then Eqn. (5.14) becomes

$$\tau_{yy}(x,0) = -\frac{B}{c}\frac{c-x}{\sqrt{c^2-x^2}} H(c-x) + \int_x^c \frac{\psi(t)dt}{\sqrt{t^2-x^2}} + x\int_x^c \frac{\phi(t)dt}{t\sqrt{t^2-x^2}}. \tag{5.15}$$

The moment, shear, and average slope are given by Eqns. (2.20), (2.21) and (2.23), respectively. As before, the beam theory solution is taken to be

$$u_y^B(x) = a_0 + a_1x + a_2x^2 + a_3x^3 \tag{5.16}$$

resulting in expressions for moment, shear and average slope given by Eqns. (2.27), (2.28) and (2.29), respectively. The constants a_1, a_2, a_3 are solved for as before, with identical outcome. Eqn. (5.5) is treated in a similar manner. Differentiating with respect to x and separating into symmetric and antisymmetric components yields

$$\left.\frac{\partial u_y^E}{\partial x}(x,0)\right|_A + 2a_2x = 0 \tag{5.17}$$

$$\left.\frac{\partial u_y^E}{\partial x}(x,0)\right|_S + a_1 + 3a_3x^2 = 0. \tag{5.18}$$

Considering each equation one at a time and following the same procedure

as before results in the following equations for A, B, $\psi(t)$ and $\phi(t)$:

$$AK_1(x,c) - \frac{h^3}{6}\psi(x) + \int_0^c \psi(t)K_1(x,t)dt + BK_2(x,c) + \int_0^c \phi(t)K_2(x,t)dt = 0 \quad (5.19)$$

$$AK_3(x,c) + \int_0^c \psi(t)K_3(x,t)dt - BK_4(x,c) + \frac{h^3}{6}\phi(x) - \int_0^c \phi(t)K_4(x,t)dt = 0 \quad (5.20)$$

where

$$K_1(x,\eta) = \int_0^\infty \{\frac{h^3}{6}(\frac{\beta+sh\beta ch\beta}{\beta^2-sh^2\beta} + 1)\xi x J_0(\xi x) + \frac{x}{\xi^2}\cos\xi(\ell-\ell_0)\}J_0(\xi\eta)d\xi + \frac{\pi}{2}x(\ell-\ell_0) \quad (5.21)$$

$$K_2(x,\eta) = \frac{\pi}{4}\eta x \quad (5.22)$$

$$K_3(x,\eta) = \frac{\pi}{4}x^2 \quad (5.23)$$

$$K_4(x,\eta) = \int_0^\infty \frac{h^3}{6}(\frac{\beta+sh\beta ch\beta}{\beta^2-sh^2\beta} + 1)\xi x J_1(\xi x)J_1(\xi\eta)d\xi \quad (5.24)$$

and $\eta = c$ or t. Eqns. (5.19), (5.20) are two equations in four unknowns. A third equation was obtained earlier by enforcing non-singularity of normal stress at $x = c$:

$$A + B = 0. \quad (5.25)$$

The fourth is found by enforcing the boundary condition given by Eqn. (5.5). After solving for the constant a_0 as before (with identical results), Eqns. (5.5), (2.15), (2.24), (5.12), (5.13) and (5.25) may be used in a manner analogous to that of solving for the displacement under the cylindrical indenter to solve for the constant B:

$$B = \frac{\Delta - \int_0^c \psi(t)K_5(t)dt - \int_0^c \phi(t)K_6(t)dt}{K_6(c) - K_5(c)} \tag{5.26}$$

where

$$K_5(n) = \frac{1-\nu}{\mu}\int_0^\infty \{(\frac{\beta+sh\beta ch\beta}{\beta^2-sh^2\beta} + 1)(\frac{1-cos\xi\ell_0}{\xi}) - \ell_0 \frac{sin\xi\ell_0}{\beta-sh\beta} - \frac{3\ell_0^2}{h^3}\frac{cos\xi(\ell-\ell_0)}{\xi^2}\}J_0(\xi n)d\xi$$

$$- \frac{1-\nu}{\mu}cosh^{-1}(\frac{\ell_0}{n}) + \frac{\pi}{4}\frac{3-2\nu}{\mu h}\ell_0 - \frac{\pi}{120}\ell_0^2(3\ell-\ell_0) \tag{5.27}$$

$$K_6(n) = \frac{1-\nu}{\mu}\int_0^\infty \{(\frac{\beta+sh\beta ch\beta}{\beta^2-sh^2\beta} + 1)\frac{sin\xi\ell_0}{\xi} - \ell_0\frac{cos\xi\ell_0}{\beta-sh\beta}\}J_1(\xi n)d\xi$$

$$- \frac{1-\nu}{\mu}\frac{n}{\ell_0+\sqrt{\ell_0^2-n^2}} - \frac{\pi n}{80}\ell_0^2 \tag{5.28}$$

and n = c or t. Making use of Eqns. (5.25), (5.26) in Eqns. (5.19), (5.20) yields

$$\frac{h^3}{6}\psi(x) - \int_0^c \psi(t)\{K_1(x,t) + \frac{K_1(x,c)-K_2(x,c)}{K_6(c) - K_5(c)}K_5(t)\}dt$$

$$- \int_0^c \phi(t)\{K_2(x,t) + \frac{K_1(x,c)-K_2(x,c)}{K_6(c) - K_5(c)}K_6(t)\}dt$$

$$= \Delta\frac{-K_1(x,c)+K_2(x,c)}{K_6(c) - K_5(c)} \tag{5.29}$$

$$\frac{h^3}{6}\phi(x) + \int_0^c \psi(t)\{K_3(x,t) + \frac{K_3(x,c)+K_4(x,c)}{K_6(c) - K_5(c)}K_5(t)\}dt$$

$$- \int_0^c \phi(t)\{K_4(x,t) - \frac{K_3(x,c)+K_4(x,c)}{K_6(c) - K_5(c)}K_6(t)\}dt$$

$$= \Delta\frac{K_3(x,c)+K_4(x,c)}{K_6(c) - K_5(c)}. \tag{5.30}$$

Thus, Eqns. (5.29), (5.30) are those used to solve for the unknown auxiliary functions $\psi(x)$, $\phi(x)$. These equations are solved numerically. Once $\psi(x)$, $\phi(x)$ are obtained, all necessary physical quantities may then be calculated.

Stresses may be calculated using Eqn. (5.15):

$$\tau_{yy}(x,0) = -\frac{B}{c}\frac{c-x}{\sqrt{c^2-x^2}}H(c-x) + \int_x^c \frac{\phi(t)dt}{\sqrt{t^2-x^2}} + x\int_x^c \frac{\phi(t)dt}{t\sqrt{t^2-x^2}} \tag{5.31}$$

where B is given by Eqn. (5.26).

The resultant load due to the symmetric stresses is found to be given by

$$P = \pi B - \pi \int_0^c \psi(t)dt. \tag{5.32}$$

The resultant moment due to the antisymmetric stresses is found to be given by

$$M = -\frac{\pi}{2} cB - \frac{\pi}{2}\int_0^c t\phi(t)dt. \tag{5.33}$$

The rotation of the beam at any point $x > c$ is found to be given by

$$\bar{\theta}(x) = B[K_3(x,c)-K_7(x,c)] - B\frac{\pi}{4}\frac{3-2\nu}{\mu h} + \int_0^c \psi(t)K_7(x,t)dt + \int_0^c \phi(t)K_8(x,t)dt \tag{5.34}$$

where

$$K_7(x,\eta) = \frac{1}{\pi}\int_0^\infty [-\frac{h^3}{6}(\frac{\sin\xi x+\sin\xi\ell_0}{\xi - \sin\xi}) - (x+\ell_0)\frac{\cos\xi(\ell-\ell_0)}{\xi^2}]J_0(\xi\eta)d\xi$$

$$- \frac{\pi}{2D} [\ell_0(\ell-\ell_0/2)+x(\ell-\ell_0)-x^2/2] + \frac{\pi}{4} \frac{3-2\nu}{\mu h} \tag{5.35}$$

$$K_8(x,\eta) = \frac{1}{D} \int_0^\infty \frac{h^3}{6} \left(\frac{\cos\xi x-\cos\xi\ell_0}{\beta - \mathrm{sh}\beta}\right) J_1(\xi\eta)d\xi - \frac{\pi}{4D} (\ell_0+x)\eta \tag{5.36}$$

and $\eta = c$ or t.

6. PROBLEM SOLUTION

Following a scheme similar to that of Sec. 3, we define

$$\alpha_1 = \ell_1/h \qquad \psi(x) = \frac{D\Delta cy}{h^5} \Psi(y) \tag{6.1), (6.2}$$

$$\phi(x) = \frac{D\Delta cy}{h^5} \Phi(y) \tag{6.3}$$

Non-dimensionalized stresses, loads, moments and rotations are calculated and may be transformed back to real quantities through

$$\tau_{yy} = P\hat{\tau}_{yy}/c \tag{6.4}$$

$$P = \mu\Delta\hat{P}/(1-\nu) \tag{6.5}$$

$$M = \mu\Delta h\hat{M}/(1-\nu) \tag{6.6}$$

$$\bar{\theta} = \Delta\hat{\bar{\theta}}/h. \tag{6.7}$$

In order to assess the accuracy of the solution obtained, two tests are performed. First, the rotation of the beam just beyond $x = c$ is compared to that given by the standard beam theory solution:

$$\bar{\theta}_B(c) = \frac{1}{2D} P(\ell_0^2-c^2) + \frac{1}{D} M(\ell_0+c) \tag{6.8}$$

where $\varepsilon = c^+$. Second, from the nature of a receding contact problem, as the contact length decreases to zero, the load P_E increases to a certain limit value. Because the moment M_E goes to zero as the contact length goes to zero, the beam theory solution for displacement tells us that the load P_E must approach the beam theory load P_{BT} for a cantilever beam problem:

$$P_{BT} = 3D\Delta/\ell_d^3 \ . \tag{6.9}$$

The limit load $\lim_{c/h\to 0} \hat{P}_E$ is compared to the value of $\hat{P}_{BT}$ for each case considered.

Once again, the use of beam theory equations in subsequent comparison studies dictates that conditions of plane stress should be assumed in the solution of Eqns. (5.29) and (5.30). As before, Poisson's ratio is taken to be equal to 0.35 for the numerical solution of these equations.

7. OBSERVATIONS AND CONCLUSIONS

Solutions to the problem were obtained for δ = 0.25, 0.5 and 1.0, γ = 10.0 and 20.0, and for each γ, ℓ = 0.25γ, 0.375γ, 0.5γ and 0.75γ. It was found that the stress distributions for the different values of ℓ/h were virtually identical. A typical distribution of the total stress under the indenter, normalized by a factor of $\sqrt{c^2-x^2}$, is shown in Fig. 5. An examination of the plots of the total stress under the indenter reveals that it is indeed singular at $x = -c$, but zero at $x = +c$. Furthermore, the stress distribution in Fig. 5 for $c/h = 1.0$ is seen to be an extreme case. This

results from a more pronounced effect of the antisymmetric component in the solution for cases where c/h is large.

Tables 6 and 8 show a comparison between the solution developed here and the classical beam theory solution. As can be seen, the elasticity solution agrees quite well with the beam theory solution. Again, it is noted that the rotations in Table 6 have no meaning unless they are converted to real values. Following the same procedure as before, an upper bound can be placed on the ratio of displacement under the indenter to beam thickness:

$$\Delta/h < \min \{\bar{\vartheta}_0/\hat{\vartheta}\,,\ (1-\nu)\sigma_y/6\mu(\alpha\hat{P}-\hat{M})\} \tag{7.1}$$

Assuming the same values of $\bar{\vartheta}_0$, σ_y and μ, Eqn. (7.1) reduces to

$$\Delta/h < 0.349/\hat{\vartheta}. \tag{7.2}$$

Under these criteria, Table 7 shows the maximum allowable values of Δ/h to ensure small rotations and no yielding.

The phenomenon of receding contact in this problem is borne out by Fig. 7. As c/h goes to zero, the non-dimensionalized load parameter approaches a limit value greater than zero. In Table 8, the limit load of the elasticity solution is seen to agree quite well with the limit load of the beam theory solution. Furthermore, the limit load is highest in those cases where the indenter is close to the wall.

In Fig. 7 the relationships between the loads and contact widths for the various cases considered appear to violate the condition imposed on receding contact problems to ensure the existence and uniqueness of their solutions [6], since, the contact lengths for a particular beam are not independent of

the applied loads on that beam. The contact length in a receding contact problem will be independent of the level of loading only if the ratio of the resultant moment to the applied load is constant for all levels of loading. In the problems solved through the course of this study, the ratio of moment to load changes as the applied loading changes; thus, the contact length will change as well, the imposed conditions are not violated, and the problems studied are indeed receding contact problems.

8. ACKNOWLEDGEMENT

The authors are grateful for support from the AFOSR (Grant AFOSR-82-0330).

References

1. Keer, L.M. and Miller, G.R., "Smooth Indentation of a Finite Layer," Journal of the Engineering Mechanics Division, ASCE, Vol. 109, 1983, pp. 706-717.

2. Keer, L.M. and Ballarini, R., "Smooth Contact between a Rigid Indenter and an Initially Stressed Orthotropic Beam," AIAA Journal, Vol. 21, 1983, pp. 1035-1042.

3. Keer, L.M. and Miller, G.R., "Contact between an Elastically Supported Circular Plate and a Rigid Indenter," International Journal of Engineering Science, Vol. 21, 1983, pp. 681-690.

4. Sneddon, I.N., Fourier Transforms, McGraw-Hill Book Co., Inc., New York, N.Y., 1951.

5. Watson, G.N., A Treatise on the Theory of Bessel Functions, 2nd Ed., Cambridge University Press, Cambridge, Great Britain, 1966.

6. Dundurs, J. and Stippes, M., "Role of Elastic Constants in Certain Contact Problems," Journal of Applied Mechanics, Vol. 37, 1970, pp. 965-970.

	$\ell/h=10.0$			$\ell/h=20.0$		
c/h	$\ell_o/h=2.5$	$\ell_o/h=5.0$	$\ell_o/h=7.5$	$\ell_o/h=5.0$	$\ell_o/h=10.0$	$\ell_o/h=15.0$
0.2	0.635	0.635	0.635	0.635	0.635	0.635
0.5	0.622	0.622	0.617	0.625	0.621	0.622
1.0	0.560	0.561	0.561	0.560	0.564	0.562

Table 1: Maximum Symmetric Stresses (Case I)

	$\ell/h=10.0$			$\ell/h=20.0$		
c/h	$\ell_o/h=2.5$	$\ell_o/h=5.0$	$\ell_o/h=7.5$	$\ell_o/h=5.0$	$\ell_o/h=10.0$	$\ell_o/h=15.0$
0.2	0.636	0.636	0.636	0.636	0.636	0.636
0.5	0.648	0.649	0.645	0.650	0.649	0.649
1.0	0.982	0.983	0.981	0.982	0.988	0.983

Table 2: Maximum Total Stresses (Case I)

$\ell/h = 10.0$	$\ell_o/h=2.5$		$\ell_o/h=5.0$		$\ell_o/h=7.5$		
	Elasticity	Beam Theory	Elasticity	Beam Theory	Elasticity	Beam Theory	c/h
	2.0	2.0	16.1	16.1	54.3	54.3	0.2
	15.5	15.3	127.3	127.5	438.6	439.0	0.5
	376.2	383.5	3487.0	3498.0	8705.0	8716.0	1.0
$\ell/h = 20.0$	$\ell_o/h=5.0$		$\ell_o/h=10.0$		$\ell_o/h=15.0$		
	Elasticity	Beam Theory	Elasticity	Beam Theory	Elasticity	Beam Theory	c/h
	16.2	16.2	127.1	127.6	435.7	435.7	0.2
	128.5	128.8	1000.0	1001.0	3466.0	3467.0	0.5
	3327.0	3338.0	35890.0	35900.0	101540.0	101570.0	1.0

Table 3: Displacement Comparison (Case I)

$\ell/h = 10.0$	$\ell_o/h=2.5$		$\ell_o/h=5.0$		$\ell_o/h=7.5$		
	Elasticity	Beam Theory	Elasticity	Beam Theory	Elasticity	Beam Theory	c/h
	1.1	1.2	4.8	4.8	10.8	10.9	0.2
	8.8	9.3	37.6	38.1	87.0	87.6	0.5
	186.4	215.9	985.8	1015.0	1683.0	1704.0	1.0
$\ell/h = 20.0$	$\ell_o/h=5.0$		$\ell_o/h=10.0$		$\ell_o/h=15.0$		
	Elasticity	Beam Theory	Elasticity	Beam Theory	Elasticity	Beam Theory	c/h
	4.8	4.9	19.0	19.1	43.5	43.6	0.2
	37.9	38.5	149.3	149.9	345.8	346.3	0.5
	940.5	969.0	5262.0	5269.0	10010.0	10040.0	1.0

Table 4: Rotation Comparison (Case I)

	$\ell/h=10.0$			$\ell/h=20.0$		
c/h	$\ell_o/h=2.5$	$\ell_o/h=5.0$	$\ell_o/h=7.5$	$\ell_o/h=5.0$	$\ell_o/h=10.0$	$\ell_o/h=15.0$
0.2	4.0	14.0	31.0	14.0	55.0	125.0
0.5	26.0	108.0	250.0	109.0	428.0	991.0
1.0	535.0	2825.0	4824.0	2695.0	15080.0	28690.0

Table 5: Minimum Allowable Values of R/h (Case I)

	$\ell_1/h=2.5$		$\ell_1/h=5.0$		$\ell_1/h=7.5$		
$\ell/h = 10.0$	Elasticity	Beam Theory	Elasticity	Beam Theory	Elasticity	Beam Theory	c/h
	0.508	0.544	0.280	0.285	0.192	0.193	0.2
	0.457	0.463	0.263	0.264	0.183	0.183	0.5
	0.403	0.303	0.239	0.219	0.172	0.166	1.0
	$\ell_1/h=5.0$		$\ell_1/h=10.0$		$\ell_1/h=15.0$		
$\ell/h = 20.0$	Elasticity	Beam Theory	Elasticity	Beam Theory	Elasticity	Beam Theory	c/h
	0.280	0.286	0.145	0.146	0.098	0.098	0.2
	0.263	0.264	0.140	0.140	0.095	0.095	0.5
	0.239	0.219	0.133	0.130	0.092	0.091	1.0

Table 6: Rotation Comparison (Case II)

	$\ell/h=10.0$			$\ell/h=20.0$		
c/h	$\ell_1/h=2.5$	$\ell_1/h=5.0$	$\ell_1/h=7.5$	$\ell_1/h=5.0$	$\ell_1/h=10.0$	$\ell_1/h=15.0$
0.2	0.68	1.24	1.81	1.24	2.39	3.54
0.5	0.76	1.32	1.90	1.32	2.48	3.63
1.0	0.86	1.46	2.02	1.46	2.62	3.82

Table 7: Maximum Allowable Values of Δ/h (Case II)

	ℓ_1/h	$\lim_{\delta\to 0} \hat{P}_E$ $(x10^{-2})$	$\hat{P}_{BT}$ $(x10^{-2})$
$\ell/h=10.0$	2.5	3.104	3.200
	5.0	0.398	0.400
	7.5	0.118	0.119
$\ell/h=20.0$	5.0	0.399	0.400
	10.0	0.049	0.050
	15.0	0.015	0.015

Table 8: Limit Load Comparison (Case II)

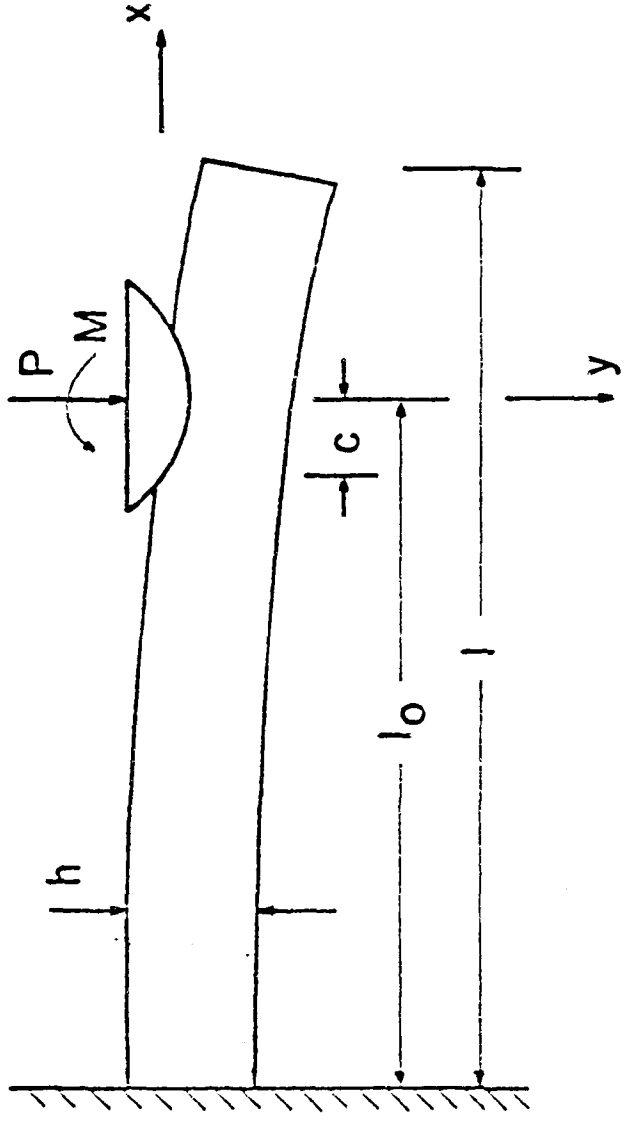

Figure 1a

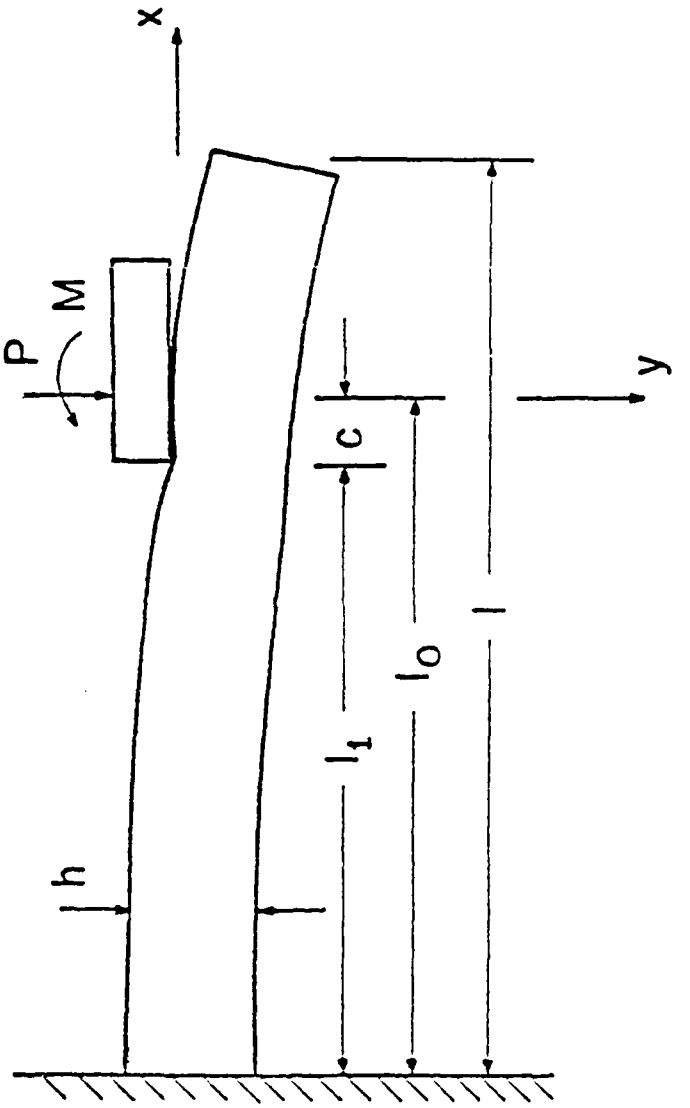

Figure 1b

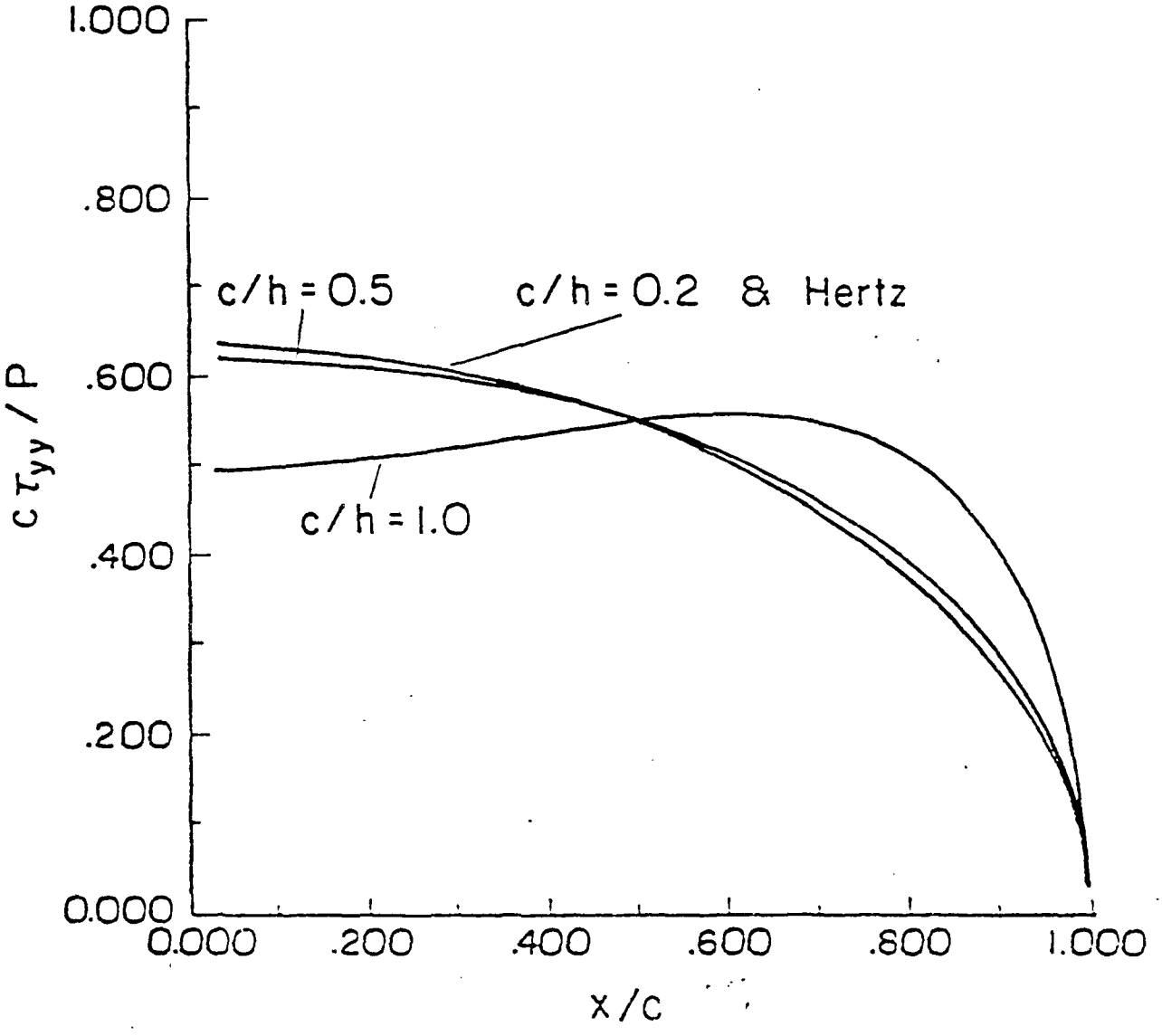
1.000
.800
.600
.400
.200
0.000
0.000
.200
.400
.600
.800
1.000
c/h = 0.5
c/h = 0.2 & Hertz
c/h = 1.0
c τyy / P
X/C

Figure 2

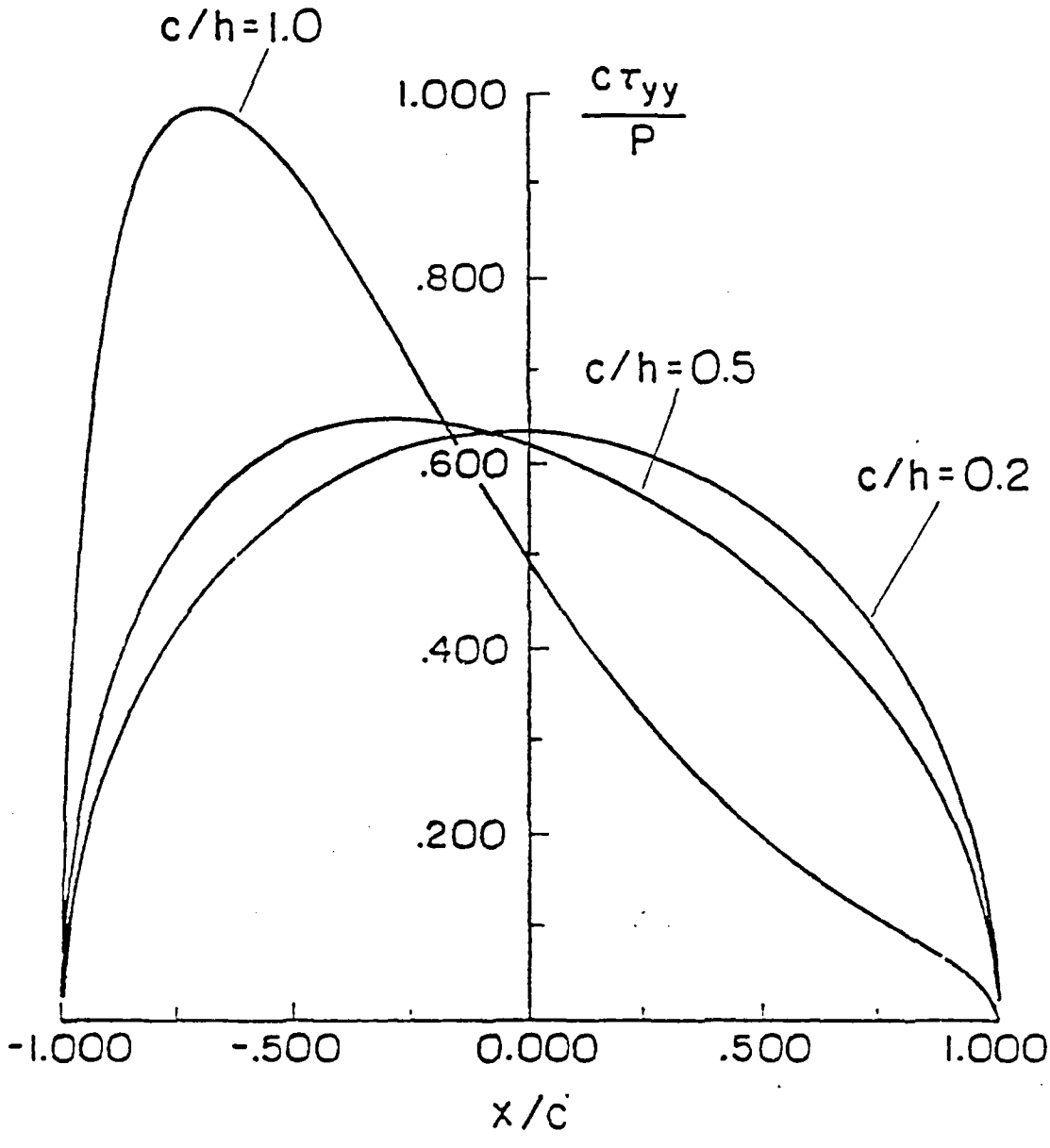
c/h=1.0
1.000
$\frac{c\tau_{yy}}{P}$
.800
c/h=0.5
.600
c/h=0.2
.400
.200
-1.000
-.500
0.000
.500
1.000
x/c

Figure 3

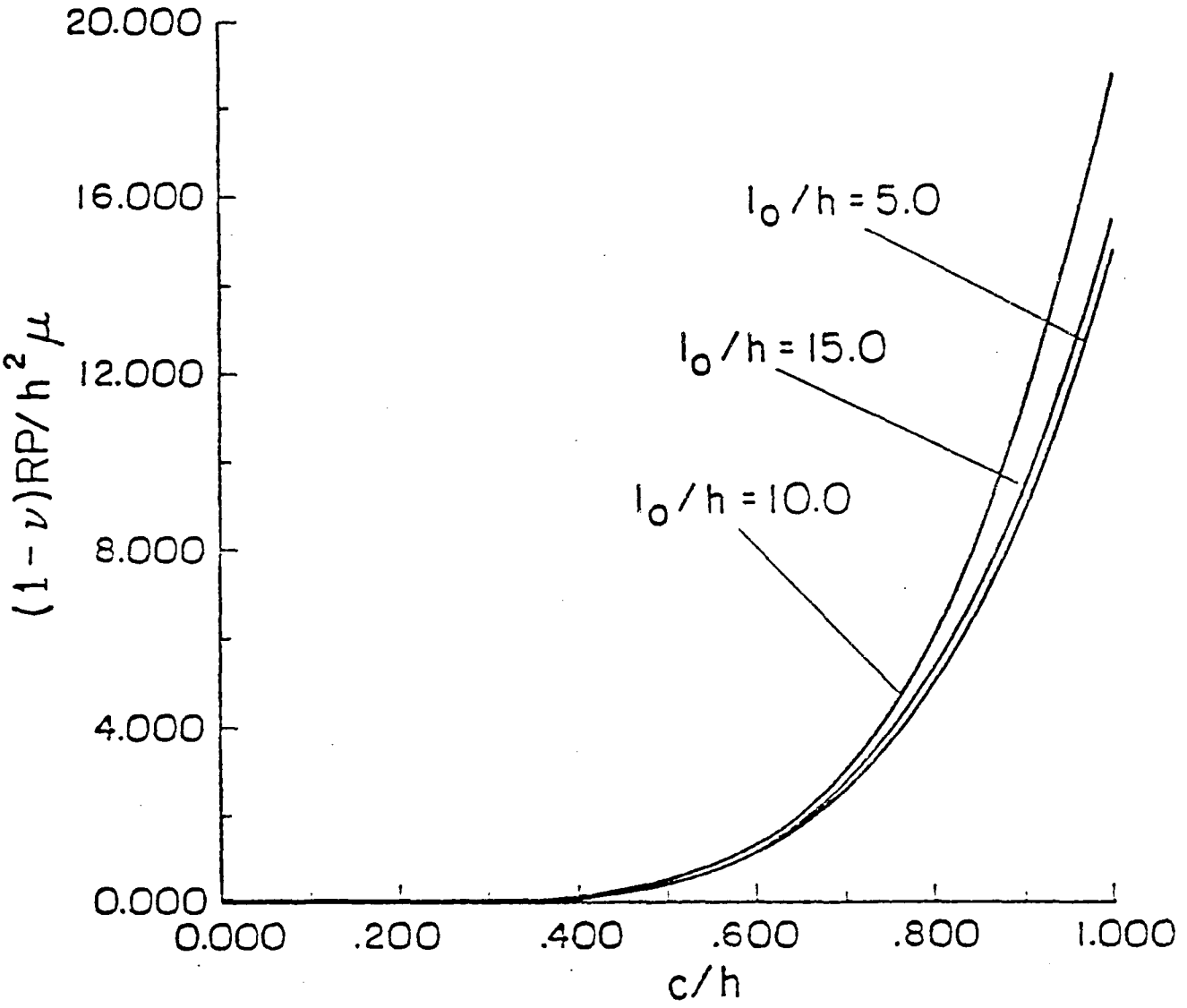
20.000
16.000
12.000
8.000
4.000
0.000
0.000
.200
.400
.600
.800
1.000
c/h
$(1-\nu)RP/h^2\mu$
$l_o/h = 5.0$
$l_o/h = 15.0$
$l_o/h = 10.0$

Figure 4

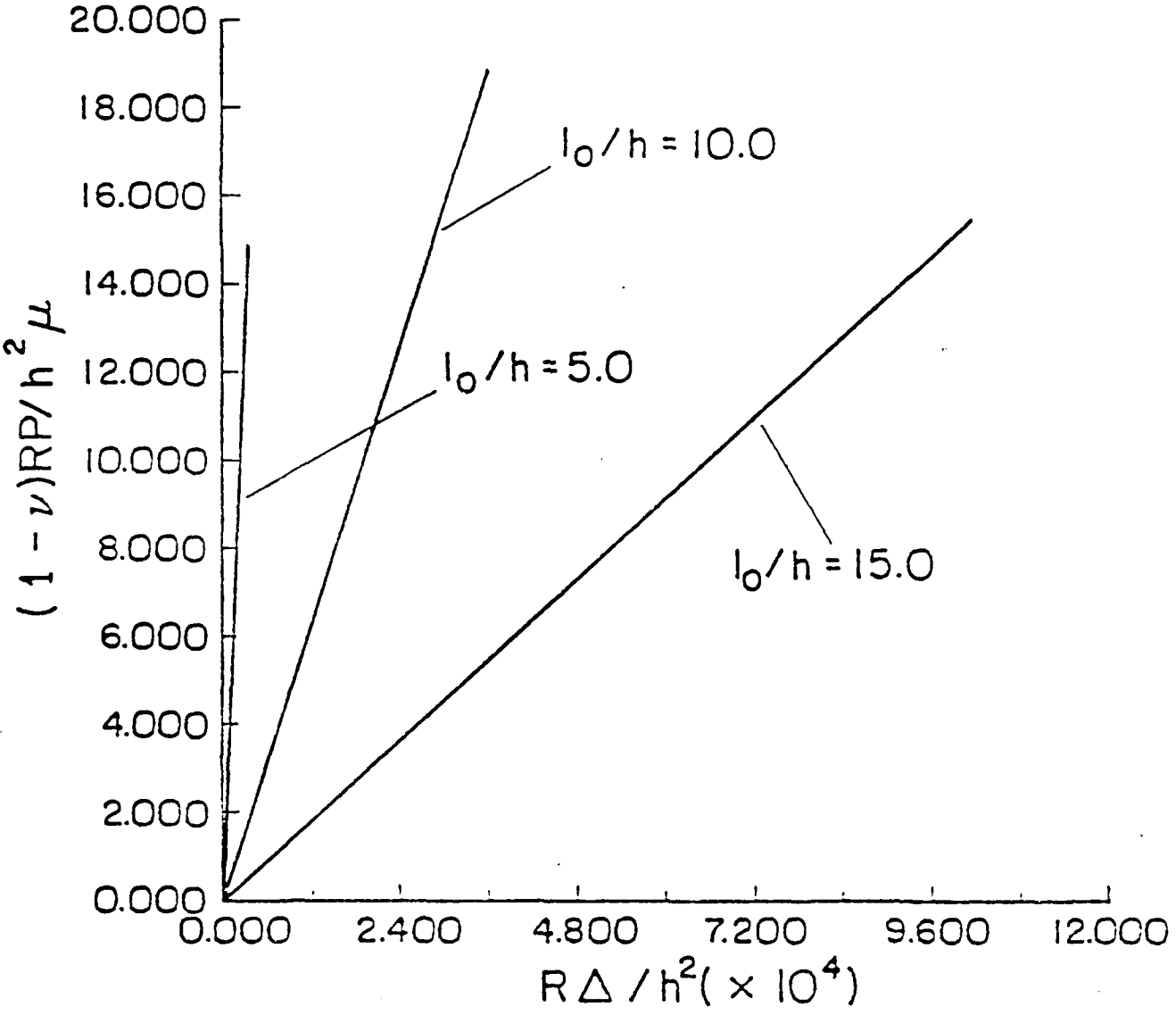

Figure 5

Load-Displacement Curve for Point

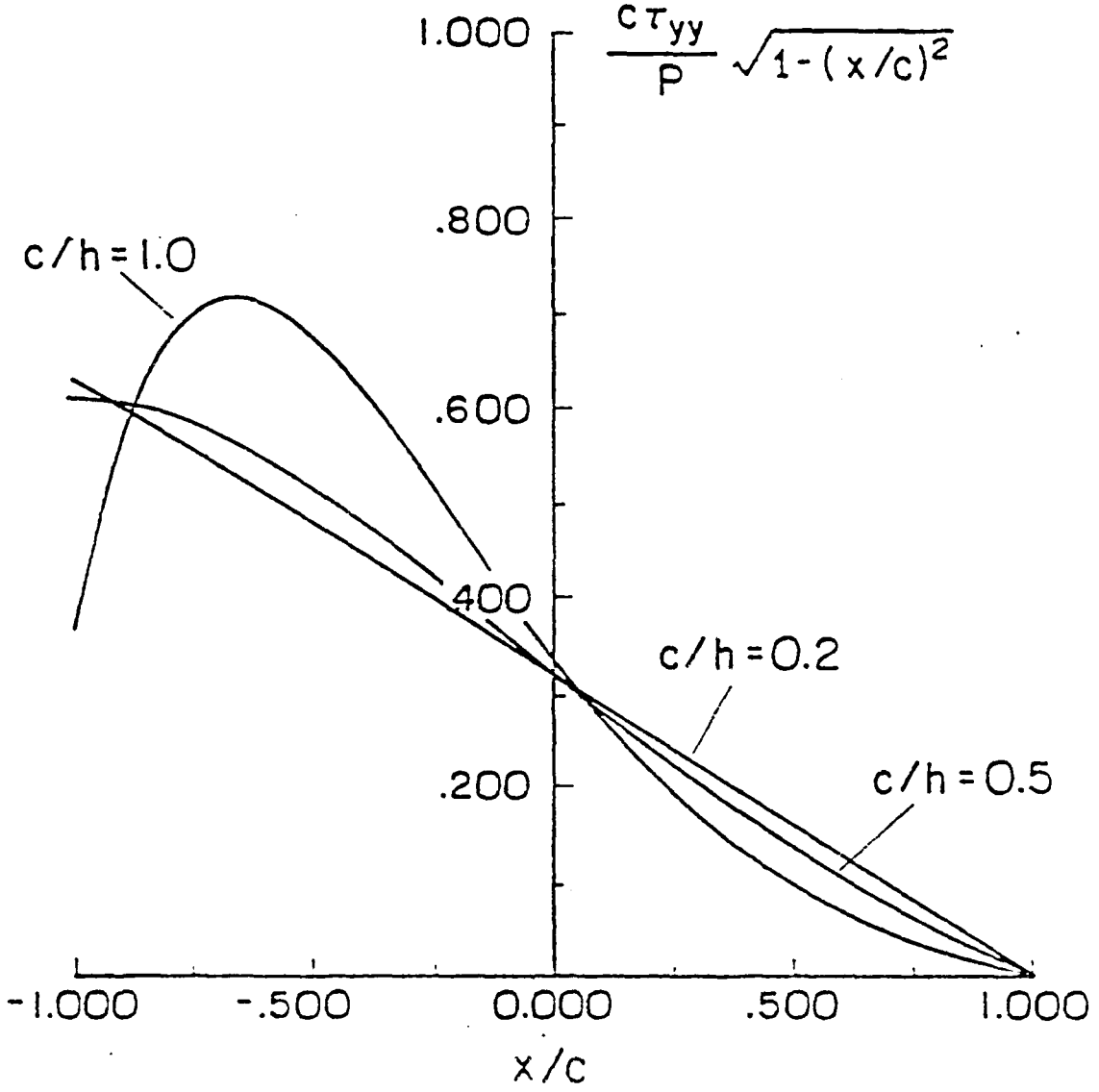
1.000
.800
.600
.400
.200
$\frac{c\tau_{yy}}{p}\sqrt{1-(x/c)^2}$
c/h = 1.0
c/h = 0.2
c/h = 0.5
-1.000
-.500
0.000
.500
1.000
x/c

Figure 6

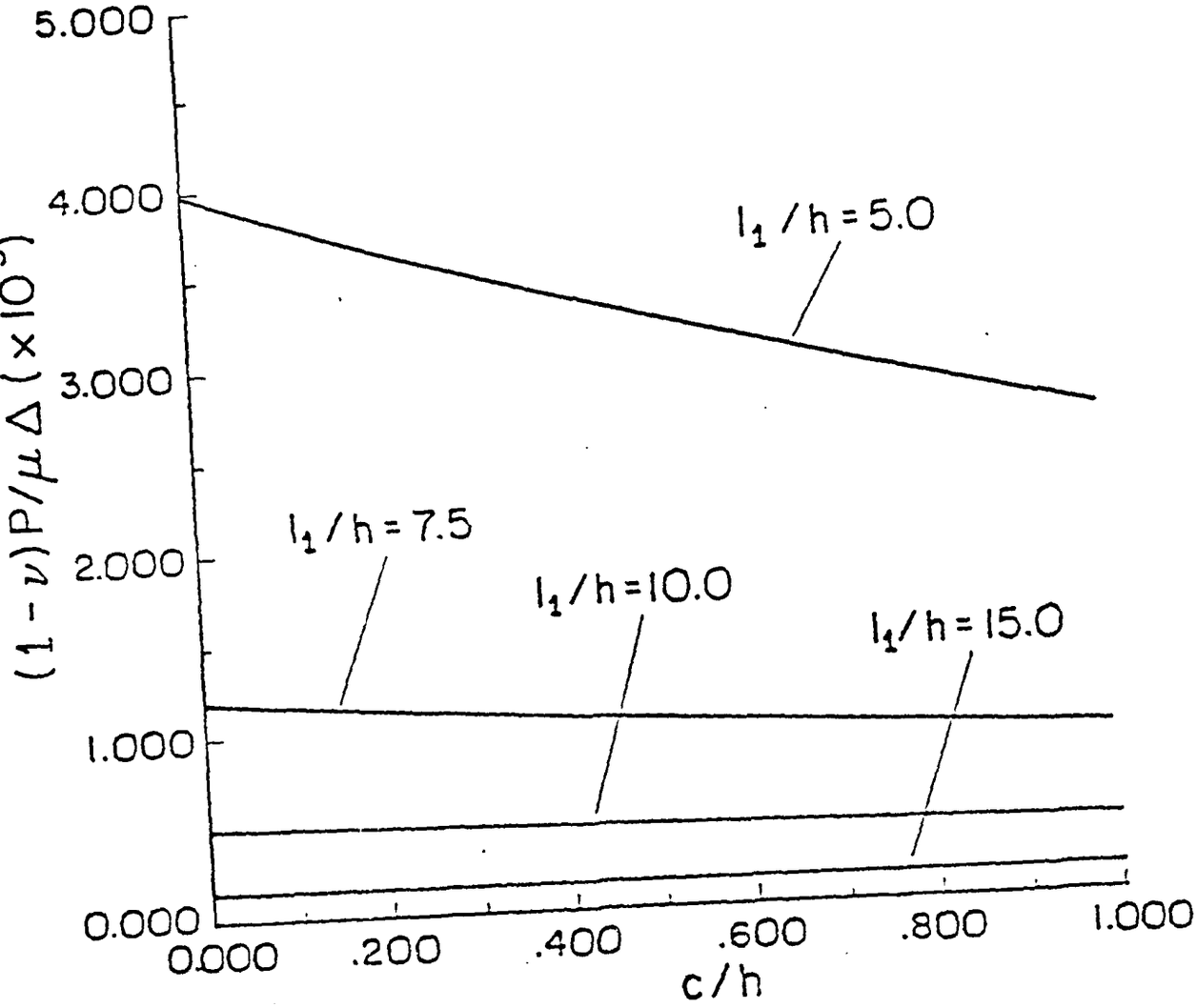
5.000
4.000
3.000
2.000
1.000
0.000
$(1-\nu)P/\mu\Delta\ (\times 10^{-3})$
$l_1/h = 5.0$
$l_1/h = 7.5$
$l_1/h = 10.0$
$l_1/h = 15.0$
0.000
.200
.400
.600
.800
1.000
c/h

Figure 7

LOW VELOCITY IMPACT ON A CIRCULAR PLATE

L. M. Keer and T. K. Woo

Department of Civil Engineering
The Technological Institute
Northwestern University
Evanston, Illinois

To Appear, Advances in Aerospace Structures, Materials and Dynamics, ASME Symposium Volume, 1984

ABSTRACT

An investigation is made on the low velocity impact on a circular plate by a rigid indenter. The plate response to impact shows some of but not all of the similar problem for a beam. The local contact stresses were developed from an elasticity theory, while the global stresses were obtained from plate theory.

INTRODUCTION

The problem of the low velocity indentation of an isotropic circular elastic plate by a rigid punch has been investigated. This study uses the assumption that an elasticity theory may be used for calculating the local effects and a Bernouilli - Euler plate theory can be used for calculating the overall dynamic response.

In this problem a spherical indenter with a very large radius of curvature strikes the plate with a low impact velocity. Since both the pressure load and contact area are unknown and depend upon time, the problem is formulated and reduced to solution of a Volterra integral equation.

Two types of solutions are superposed. One is the static solution analagous to the one developed by Keer and Miller [1]; the other is a standard dynamic plate solution which can be obtained from Bernouilli - Euler plate analysis (see e.g. Graff [2]).

The pressure distribution is assumed to be piecewise constant. Incorporating both static and dynamic solutions, the pressure distribution can be solved. The technique that was developed by Ahmadi, Keer and Mura [3] for the solution of a non-metzian contact problem was used to solve for the [illegible] contact pressure. All the field quantities can be obtained once

the time wise pressure distribution is calculated. An example for the case of plane strains low velocity has been given in an earlier paper by Keer and Lee [4].

PROBLEM FORMULATION

The formulation uses the assumption that elastodynamic effects are negligible when compared with the effects due to the static deformation. However, dynamic effects are incorporated into the plate bending solution. The solution of this problem is obtained by superposition of the static solution with a dynamic plate solution.

The boundary condition for an elastically supported layer loaded by a smooth rigid indenter are as follows:

$$\tau_{zz}(r,h) = 0 \qquad 0 \leq r < \infty \qquad (1)$$

$$\tau_{zr}(r,h) = 0 \qquad 0 \leq r < \infty \qquad (2)$$

$$\tau_{zr}(r,o) = 0 \qquad 0 \leq r < \infty \qquad (3)$$

$$\tau_{zz}(r,o) = 0 \qquad c < r < \infty \qquad (4)$$

$$\tau_{zz}(r,o) = -p(r) \qquad 0 \leq r \leq c \qquad (5)$$

where c is the radius of the contact area.

The boundary conditions at the ends of the plate are:

$$u_z = 0 \qquad r = a \qquad (6)$$

$$M + K\bar{\beta} = 0 \qquad r = a \qquad (7)$$

where a is the radius of the plate, M is the moment, K is spring constant, and $\bar{\beta}$ is the value of the slope averaged through the thickness.

$$\bar{\beta} = \frac{1}{h}\int_0^h \frac{\partial u_r}{\partial z}\, dz \qquad (8)$$

The elasticity solution that represents loading on the upper surface of an elastic layer is given in the following form by use of integral transforms:

$$2\mu u_r = \int_0^\infty \frac{E(\xi)}{\Delta} \{[(1-2\nu)(\beta + sh\beta ch\beta) - \xi z sh^2\beta]sh(\xi z)$$

$$- [(1-2\nu)sh^2\beta + \beta^2 - \xi z(\beta + sh\beta ch\beta)ch(\xi z)\}$$

$$\times J_1(\xi r)d\xi \qquad (9)$$

$$2\mu u_z = - \int_0^\infty \frac{E(\xi)}{\Delta} \{[2(1-\nu)sh^2\beta - \beta^2 + \xi z$$

$$(\beta + sh\beta ch\beta]sh(\xi z) - [2(1-\nu)(\beta + sh\beta ch\beta)$$

$$- \xi z sh^2\beta]ch(\xi z)\}J_0(\xi r)d\xi \qquad (10)$$

$$\tau_{rr} = \int_0^\infty \frac{\xi E(\xi)}{\Delta} \{[\xi z - \beta - sh\beta ch\beta]sh(\xi z)$$

$$+ [\beta^2 + sh^2\beta - \xi z(\beta + sh\beta ch\beta)]ch(\xi z)]J_0(\xi r)d\xi$$

$$- \frac{1}{r}\int_0^\infty \frac{\xi E(\xi)}{\Delta} \{[\beta^2 + (1 - 2\nu)sh^2\beta - \xi z$$

$$[\beta + sh\beta ch\beta)]ch(\xi z) + [\xi z sh^2\beta$$

$$- (1-2\nu)\ (\beta + sh\beta ch\beta)]sh(\xi z)\}J_1(\xi r)d\xi \qquad (11)$$

$$\tau_{rz} = \int_0^\infty \frac{\xi E(\xi)}{\Delta} \{[\beta^2 - \xi z(\beta + sh\beta ch\beta)]sh(\xi z)$$

$$+ [\xi z sh^2\beta]ch(\xi z)\}J_1(\xi r)d\xi \qquad (12)$$

$$\tau_{zz} = \int_0^\infty \frac{\xi E(\xi)}{\Delta} \{[\beta + sh\beta ch\beta + \xi z sh^2\beta]sh(\xi z)$$

$$- [\xi z(\beta + sh\beta ch\beta) + sh^2\beta - \beta^2]ch(\xi z)\}J_0(\xi r)d\xi \qquad (13)$$

where Δ = [illegible] - sh[illegible], [illegible] and [illegible] are shear modulus and Poisson's Ratio. Here, sh [illegible] and ch [illegible] refer to hyperbolic sine and cosine, respectively.

Both the normal and shear stress vanish at $z = h$, but at $z = 0$, the shear stress is zero, the normal stress is given as

$$\sigma_{zz}(r,0) = \int_0^\infty E(\xi)\,\xi J_0(\xi r)\,d\xi \tag{14}$$

By applying boundary condition [illegible] and Hankel transform,

$$E(\xi) = -\int_0^c rP(r)\,J_0(\xi r)\,dr \tag{15}$$

Taking the quadratic displacement (constant moment solution) as in the plate solution by Keer and Miller [1],

$$u_z = Ar^2 + B \tag{16}$$

where

$$A = \frac{-M_L(L)}{2D(1+\nu)} \; ; \; D = \frac{Eh^3}{12(1-\nu^2)} \tag{17}$$

To determine the constant A, we first derive the moment and average slope representation due to the layer solution in such a manner that the end conditions can be met. Thus,

$$M_L(L) = \int_0^h \sigma_{rr}\big|_{r=a}\, z\,dz = -\int_0^\infty \frac{E(\xi)}{\xi}\, J_0(\xi a)\,d\xi \ldots$$

[illegible]

$$\theta_L(L) \equiv \frac{1}{h}\int_0^h \frac{\partial u_z}{\partial r}\Big|_{r=a} dz = -\frac{1}{2\mu h}\int_0^\infty E(\xi)$$

$$\left(\frac{\beta - (3 - 2\nu)sh\beta}{\beta - sh\beta}\right) J_1(\xi a)\, d\xi \qquad (19)$$

By using (7), (17), (18), (19), A is determined to be

$$A = \frac{1}{2D(1 + \nu + \alpha)}\int_0^\infty E(\xi)\left\{-\frac{J_0(\xi a)}{\xi}\right.$$

$$+ \frac{1}{a\xi^2}\left[1 + 2\nu\left(\frac{\beta^2 ch\beta - sh^2\beta}{\beta^2 - sh^2\beta}\right)\right]J_1(\xi a)$$

$$\left. + \frac{h^2\alpha}{12(1 - \nu)a}\left(\frac{\beta - (3 - 2\nu)sh\beta}{\beta - sh\beta}\right)J_1(\xi a)\right\}d\xi \qquad (20)$$

The constant B can be determined in a similar way

$$B = -\frac{1}{D}\int_0^\infty E(\xi)\left\{\frac{h^3}{D}\left(\frac{\beta + sh\beta ch\beta}{\beta^2 - sh^2\beta}\right)J_0(\xi a)\right.$$

$$\left. - \frac{a^2}{2(1 + \alpha - \nu)}\, Q(\xi)\right\}d\xi \qquad (21)$$

where

$$Q(\xi) = \frac{J_0(\xi a)}{\xi} - \frac{1}{a\xi^2}\left[1 + 2\nu\left(\frac{\beta^2 sh\beta - sh^2\beta}{\beta^2 - sh^2\beta}\right)\right]J_1(\xi a)$$

$$+ \frac{h^2\alpha}{12(1 - \nu)a}\left(\frac{\beta - (3 - 2\nu)sh\beta}{\beta - sh\beta}\right)J_1(\xi a) \qquad (22)$$

[illegible]

From equations (10), (15), (16), (20), and (22)

$$u_z = \frac{1}{2D}\int_0^c r'p(r')dr' \int_0^\infty J_0(\xi r')\left\{\frac{h^3}{3}\,\frac{\beta + \mathrm{sh}\beta\mathrm{ch}\beta}{\beta^2\mathrm{sh}^2\beta}\right.$$

$$\times\ (J_0(\xi a) - J_0(\xi r)) - \frac{a^2 - r^2}{1 + \alpha + \nu}\left\{\frac{Jo(\xi a)}{\xi}\right.$$

$$- \frac{1}{a\xi^2}\left(1 + 2\nu\left(\frac{\beta^2\mathrm{ch}\beta - \mathrm{sh}^2\beta}{\beta^2 - \mathrm{sh}^2\beta}\right)\right)J_1(\xi a)$$

$$\left.\left. + \frac{h^2\alpha}{12(1 - \nu)a}\left(\frac{\beta - (3 - 2\nu)\mathrm{sh}\beta}{\beta - \mathrm{sh}\beta}\right)J_1(\xi a)\right\}\right\}d\xi \qquad (23)$$

As $\xi \to 0$, an asymptotic analysis shows the terms in equation (23) to be bounded. However, as $\xi \to \infty$, the terms are divergent. By adding and subtracting

$$\frac{1}{2D}\int_0^c r'p(r')dr' \int_0^\infty \frac{h^3}{3}(J_0(\xi a) - J_0(\xi r))d\xi \qquad (24)$$

$$\times\ \frac{(3-2\nu)}{2D}\,\frac{a^2 - r^2}{1 + \alpha + \nu}\,\frac{h^2\alpha}{12(1 - \nu)a}\int_0^c r'p(r')$$

$$\times \int_0^\infty J_0(\xi r')J_1(\xi a)d\xi dr' \qquad (25)$$

the difficulty can be removed.

DYNAMIC PLATE THEORY SOLUTION

A solution can be obtained by using a normal mode expansion together with a Laplace transform. The equation governing the normal mode expansion is given as

$$\nabla^4\psi_n(r) - \beta_n^4\psi_n(r) = 0 \qquad (26)$$

where $Y_n(r)$ are the mode shapes and ∇^4 is the biharmonic operator. The solution can be written as $Y_n = Y_1 + Y_2$ where Y_1, Y_2 satisfy respectively

$$\nabla^2 Y_1 + \beta_n^2 Y_1 = 0 \ , \ \nabla^2 Y_1 - \beta_n^2 Y_2 = 0 \qquad (27)$$

where ∇^2 is the Laplace operator. Because of axial symmetry, we obtain

$$Y_1'' + \frac{1}{r} Y_1' + \beta_n^2 Y_1 = 0$$

which has the solution

$$Y_1 = AJ_0(\beta_n r) + BY_0(\beta_n r) \qquad (28)$$

Similarly,

$$Y_2'' + \frac{1}{r} Y_2' - \beta_n^2 Y_2 = 0$$

which has the solution

$$Y_2 = CI_0(\beta_n r) + DK_0(\beta_n r) \qquad (29)$$

The total solution is thus,

$$Y_n(r) = (AJ_0(\beta_n r) + BY_0(\beta_n r) + CI_0(\beta_n r)$$

$$+ DK_0(\beta_n r) \qquad (30)$$

Since both Y_0, K_0 have a singularity at $r = 0$, they must be set to zero. Thus, the solution is reduced to

$$Y_n(r) = \{AJ_0(\beta_n r) + CI_0(\beta_n r)\} \tag{31}$$

For the clamped case

$$Y_n(a) = \frac{\partial Y_n(a)}{\partial r} = 0 \tag{32}$$

Substituting into equation (31), we get the frequency equation

$$I_0(\beta_n a)J_0'(\beta_n a) - J_0(\beta_n a)I_0'(\beta_n a) = 0 \tag{33}$$

and the normal mode

$$Y_n(r) = \{J_0(\beta_n r) - \frac{J_0(\beta_n a)}{I_0(\beta_n a)} I_0(\beta_n r)\} \tag{34}$$

For the simply supported case, the boundary conditions are

$$Y_n(a) = 0 \qquad \text{at } r = a \tag{35}$$

$$M = 0 \qquad \text{at } r = a \tag{36}$$

From boundary conditions (35) and (36) the frequency equation and normal mode are

$$I_0(\beta_n a)J_0''(\beta_n a) - J_0(\beta_n a)I_0''(\beta_n a)$$

$$- I_1(\beta_n a)\ J_1(\beta_n a) = 0 \tag{37}$$

$$Y_n = J_0(\beta_n r) - \frac{J_0(\beta_n a)}{I_0(\beta_n a)}\ I_0(\beta_n r) \tag{38}$$

To derive the dynamically loaded solution, we take the Laplace transform of the governing equation,

$$D\left(\frac{\partial^2}{\partial r^2} + \frac{1}{r}\frac{\partial}{\partial r}\right)^2 Y(r) + \rho h \frac{\partial^2 Y(r)}{\partial t^2} = p(r,t) \tag{39}$$

where

$$G^2 = \frac{D}{\rho h}$$

The Laplace transform of (39) is

$$G^2\left(\frac{\partial^2}{\partial r^2} + \frac{1}{r}\frac{\partial}{\partial r}\right)^2 \bar{Y}(r,s) + s^2 \bar{Y}(r,s) = \bar{p}(r,s)/\rho h \tag{40}$$

and the transform, $\bar{Y}(r,s)$, $\bar{p}(r,s)$ may be expanded in a series of normal modes $Y_n(r)$ as

$$\bar{Y}(r,s) = \sum_{n=1}^{\infty} a_n(s) Y_n(r)\ ,$$

$$\bar{p}(r,s) = \sum_{n=1}^{\infty} b_n(s) Y_n(r) \tag{41}$$

We get from orthogonality

$$b_n(s) = \tfrac{1}{2}a^2[(J_0^2(a\beta_n) + (J_0'^2(a\beta_n)]^{-1}$$

$$\times \int_0^a r\bar{p}(r,s)Y_n(r)dr \qquad (42)$$

where $Y_n(r)$ is the solution of

$$\nabla^4 Y_n(r) - \beta_n^4 Y_n(r) = 0 \qquad (43)$$

Recalling that

$$G^2\left(\frac{\partial^2}{\partial r^2} + \frac{1}{r}\frac{\partial}{\partial r}\right)^2 \sum_{n=1}^{\infty} a_n Y_n(r) + s^2 \sum_{n=1}^{\infty} a_n Y_n(r)$$

$$= \frac{1}{\rho h} \sum_{n=1}^{\infty} b_n Y_n(r) \qquad (44)$$

we have from (41)

$$G^2 \sum_{n=1}^{\infty} \beta_n^4 a_n Y_n(r) + s^2 \sum_{n=1}^{\infty} a_n Y_n(r)$$

$$= \frac{1}{\rho h} \sum_{n=1}^{\infty} b_n Y_n(r) \qquad (45)$$

Since

$$\sum_{n=1}^{\infty} (\beta_n^4 G^2 + s^2) a_n Y_n(r) = \frac{1}{\rho h} \sum_{n=1}^{\infty} b_n Y_n(r) , \qquad (46)$$

a_n can be determined as

$$a_n = \frac{b_n(s)}{\rho h(\beta_n^4 G^2 + s^2)} \qquad (47)$$

and

$$Y(r,s) = \frac{1}{\rho h} \frac{1}{a^2\{(J_0^2(a\beta_n) + J_0'^2(a\beta_n)\}} \sum_{n=1}^{\infty} \frac{Y_n(r)}{G^2\beta_n^4 + s^2}$$

$$\times \int_0^a \gamma\bar{p}(r,s)Y_n(r)dr \tag{48}$$

Since,

$$\mathcal{L}^{-1}\left(\frac{1}{s^2 + G^2\beta_n^4}\right) = \frac{1}{G\beta_n^2} \sin G\beta_n^2 t \tag{49}$$

from (48), (49)

$$Y(r,t) = \frac{1}{\rho h} \frac{1}{G\beta_n^2} \frac{Y_n(r)}{a^2\{J_0^2(a\beta_n) + J_0'^2(a\beta_n)\}}$$

$$\times \int_0^a r'Y_n(r') \int_0^t p(u,\xi) \sin G\beta_n^2 (t - \xi)d\xi dr' \tag{50}$$

INTEGRAL EQUATION FORMULATION

The integral equation to be solved is a Volterra integral equation given as

$$u_z = \frac{1}{2D} \int_0^c r'p(r') \; \int_0^\infty J_0(\xi r') \frac{h^2}{3} \frac{[illegible]}{[illegible]}$$

$$\times (J_0(\xi a) - J_0(\xi r)) - \frac{a^2 - r^2}{1 + \alpha\nu} \frac{J_0(\xi a)}{\xi}$$

$$- \frac{1}{a\xi^2} (1 + 2\nu)\left(\frac{\beta^2 ch\beta - sh^2\beta}{\beta^2 - sh^2\beta}\right)) J_1(\xi a)$$

$$J_1(\xi a)$$

$$+ \frac{h^2\alpha}{12(1 - \nu)a} \left(\frac{\beta - (3 - 2\nu)sh\beta}{\beta - sh\beta}\right) J_1(\xi a)]\}d\xi dr'$$

$$+ \sum_{n=1}^{\infty} \frac{1}{\rho h} \frac{1}{G\beta_n^2} \frac{Y_n(r)}{a^2[J_0^2(a\beta_n) + J_0^2(a\beta_n)]}$$

$$\times \int_0^a r'Y_n(r') \int_0^t p(u,\xi) \sin G\beta_n^2 (t - \xi)d\xi dr' \quad (51)$$

In the contact region we have

$$u_z(r,t) = \delta(t) - \frac{r^2}{2R} \qquad 0 < r < c(t) \qquad (52)$$

where $\delta(t)$ is the relative approach and R is the radius of curvature of the striker.

From Newton's equation of motion

$$\delta(t) = Vt - \frac{2M}{\rho h a^2} \int_0^t (t - \xi) \int_0^{c(\xi)} rp(r,\xi)drd\xi \quad (53)$$

where V is the velocity of the striker as it hits the plate and M is the ratio of the mass of the plate to that of the striker. The method to determine the unknown contact area is given in Ahmadi, et. al. [3].

NUMERICAL SOLUTION AND RESULTS

In solving the integral equation (52), some techniques have been used to take care of the singularity and speed of convergence. Third order polynomials are used to approximate the unknown function, since increasing the order of polynomial to higher order does not mean that better accuracy will be achieved. Filon's formula is used to improve the accuracy of the trignometrical parts of the kernal. The overestimated contact area and modified starting value of the Volterra integral equation help to ensure the accuracy of the numerical results.

Calculations are based on a variety of geometrical and material parameters. They are the following:

Radius of Striker:	40 cm
Radius of Plate:	10 cm
Elasticity Constant:	200 Gpa
Thickness of Plate:	1 cm
Poisson's Ratio:	0.25
Density of Plate:	7.8335 g/cm^3

Figures 2-3 show the contact area and contact force for cases of different velocities and mass ratios. As the mass ratio is increased the period of impact becomes shorter; however, changing the initial velocity does not appear to affect the period of impact. By comparing with Keer and Lee [4], the period of impact for the plate is shorter than that of the beam. This is considered to be due to the stronger boundary effect in the three-dimensional problem. As mass ratio increases, the maximum force shifts from the first peak to the second peak, although the double peaks are not so

prominent as in [4]. The pressure distribution is shown in Fig. 4-7, which corresponds to several values of the mass ratio. The non-Hertzian solution begins to appear in Fig. 4, and the wrapping effect, Keer and Miller [1], becomes more important. The pressure distribution begins to concentrate more closely to the edge of the contact than the center.

Figures 8 - 10 show the pressure distribution for different velocities. It is seen that the ratio of the peak forces tends to be proportional to the ratio of velocities. The shape of the force history and contact area are very similar for these cases.

Figure 11 shows the pressure distribution for the impact of a clamped plate by a striker with velocity 20 m/s and a mass ratio 1. As can be seen the rate of increase of the force is the same as in the case of the simple support plate. Non-Hertzian solution occurs during a portion of the impact time. The period of impact is noticeably shorter since the clamped plate is stiffer.

Figure 12 shows the force history and contact length when the thickness of the plate is 0.125 cm. As the plate becomes less stiff, we observe a double strike phenomenon, similar to that noted by Keer and Lee [4] for the related beam problem. The velocity of the striker fortties case has been reduced to 2 m/s to make elastic behavior assumption valued as the thickness of the plate is reduced. Figures 13, to 14 show the pressure distribution for this reduced thickness case. At the timewise point near detachment, the plate experienced as rather high stress.

CONCLUSION

We note that these results do not show the double strike phenomenon that we found in our two-dimensional paper by Keer and Lee [4], for a similar

geometry. However, the double strike phenomenon can still occur if the plate is sufficiently soft. Related observations to our results are calculated in Goldsmith [6]. For $M = 0.75$ and relatively thick plates the relation between force and time is noted to be nearly constant for a portion of the time. Parameters such as these may prove to be useful for the design of an impact test in which the force is kept relatively constant during a prescribed period of time.

ACKNOWLEDGEMENT

The authors are grateful for support from the Air Force Office of Scientific Research Grant AFOSR 82-0330

REFERENCES

1. Keer, L.M. and Miller, G.R., "Contact Between an Elastically Supported Circular Plate and a Rigid Indenter," International Journal of Engineering Science, Vol. 21, No. 6, 1983.

2. Graff, K.F., Wave Motion in Elastic Solids, Ohio State University Press, 1975.

3. Ahmadi, N., Keer, L.M., and Mura, T., "Non-Hertzian Stress Analysis--Normal and Sliding Contact," International Journal of Solids and Structures, Vol. 19, 1983, pp. 357-373.

4. Keer, L.M. and Lee, J.C., "Dynamic Impact of an Elastically Supported Beam--Large Area Contact", International Journal of Engineering Science, in press.

5. Goldsmith, W., Impact, The Theory and Physical Behavior of Colliding Solids, Edward Arnold Ltd., London, 1960.

Figure Captions

Fig. 1: Geometry for Circular Plate Loaded by Rigid Indenter

Fig. 2: Contact Lenth Vs. Time for Simply Supported Plate Subjected to Impact (v = 20 m/s)

Fig. 3: Force History for Simply Supported Plate Subjected to Impact (v = 20 m/s)

Fig. 4: Pressure Distribution for Simply Supported Plate (M = 0.75, v = 20 m/s)

Fig. 5: Pressure Distribution for Simply Supported Plate (M = 1.0, v = 20 m/s)

Fig. 6: Pressure Distribution for Simply Supported Plate (M = 1.5, v = 20 m/s)

Fig. 7: Pressure Distribution for Simply Supported Plate (M = 2.0, v = 20 m/s)

Fig. 8: Pressure Distribution for Simply Supported Plate (M = 1.0, v = 15 m/s)

Fig. 9(a): Force History for Simply Supported Plate Subjected to Impact (M= 1.0)

Fig. 9(b): Contact Length vs. Time for Simply Supported Plate Subjected to Impact (M = 1.0)

Fig. 10: Pressure Distribution for Clamped Plate (v = 20 m/s, M = 1.0)

Fig 11(a): Contact Length vs. Time for Clamped Plate Subjected to Transverse Impact (v = 20 m/s, M = 1.0)

Fig 11(b): Force History for Clamped Plate Subjected to Transverse Impact (v = 20 m/s, m = 1.0)

Fig 12(a): Force History for Simply Supported Plate Subjected to Impact (V = 2 m/s. Thickness of Plate = 0.125 cm)

Fig 12 b): Contact Length vs Time for Simply Supported Plate Subjected to Impact (V = 2 m/s. Thickness of Plate = 0.125 cm)

Fig 13: Pressure Distribution for Simply Supported Plate (M = 1.0, V = 2 m/s. Thickness of Plate = 0.125 cm)

Fig 14: Pressure Distribution for Simply Supported Plate (M = 1.5, V = 2 m/s. Thickness of Plate = 0.125 cm)

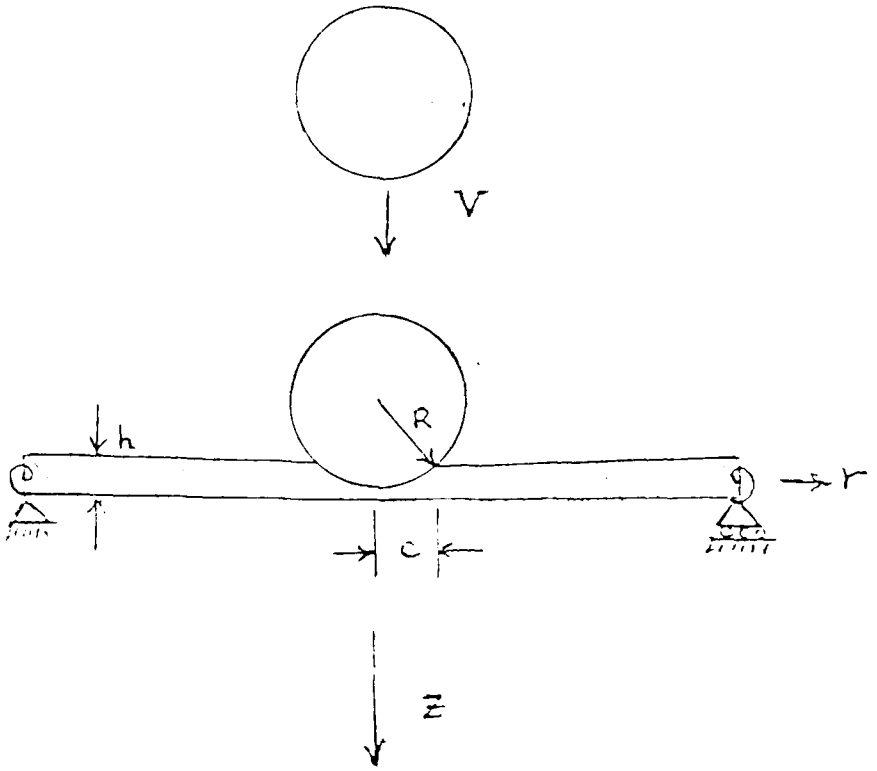

Fig. 1: Geometry for Circular Plate Loaded by Rigid Indenter

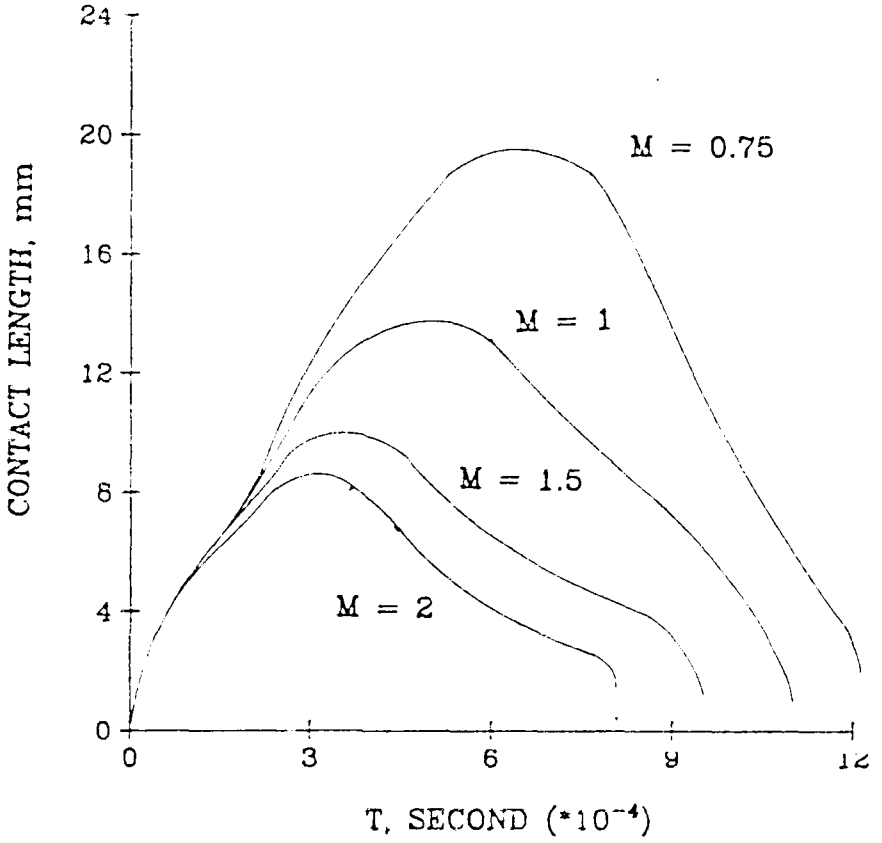
CONTACT LENGTH, mm
24
20
16
12
8
4
0
M = 0.75
M = 1
M = 1.5
M = 2
0
3
6
9
12
T, SECOND (*10⁻⁴)

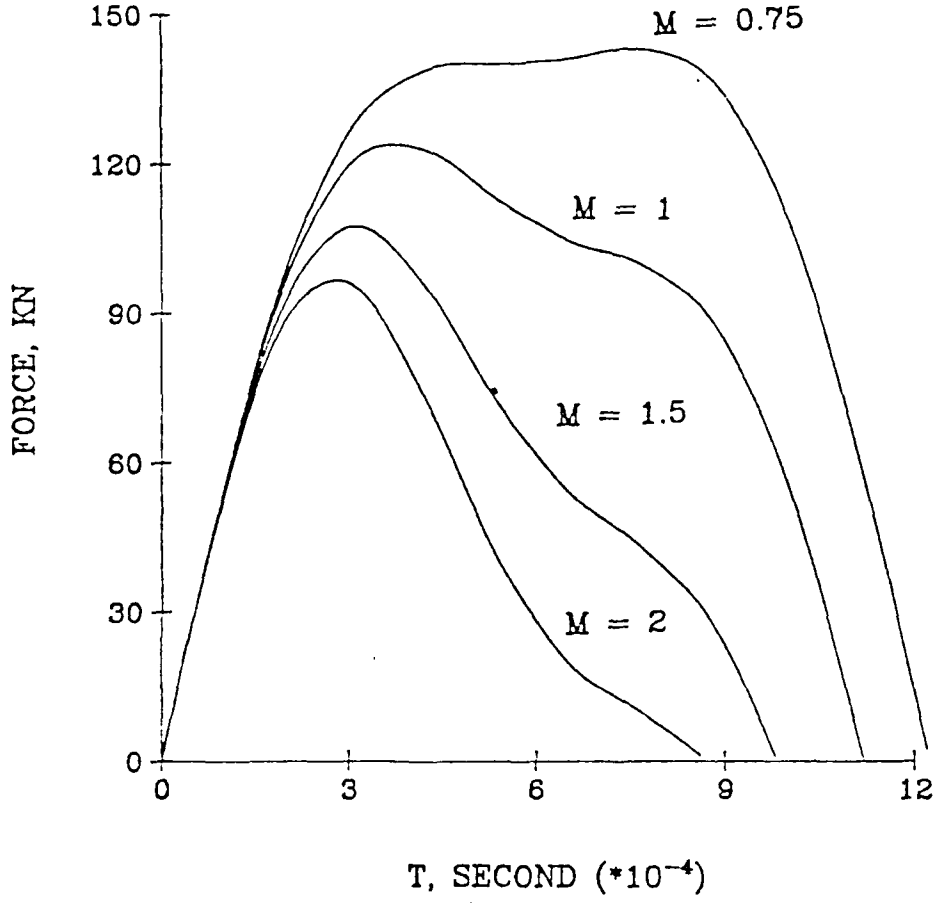

Fig. 3: Force History for Simply Supported Plate Subjected to Impact (V = 20 m/s)

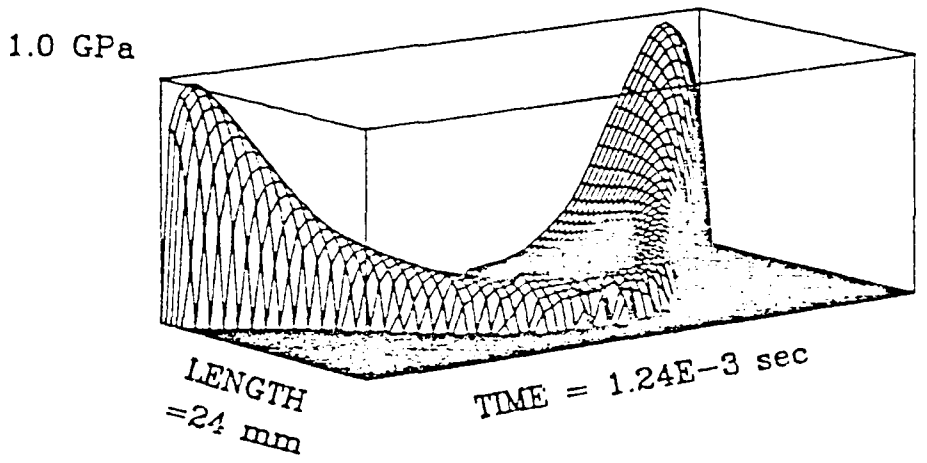

Fig. 4: Pressure Distribution for Simply Supported Plate (M = 0.75, V = 20 m/s)

Note: M is the ratio of the mass of the plate to the mass of the striker

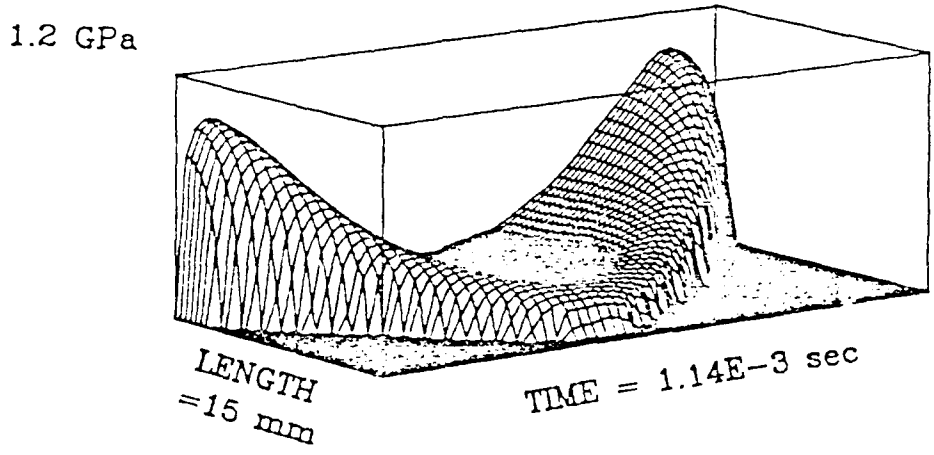

Fig. 5: Pressure Distribution for
Simply Supported Plate
(M = 1.0, V = 20 m/s)

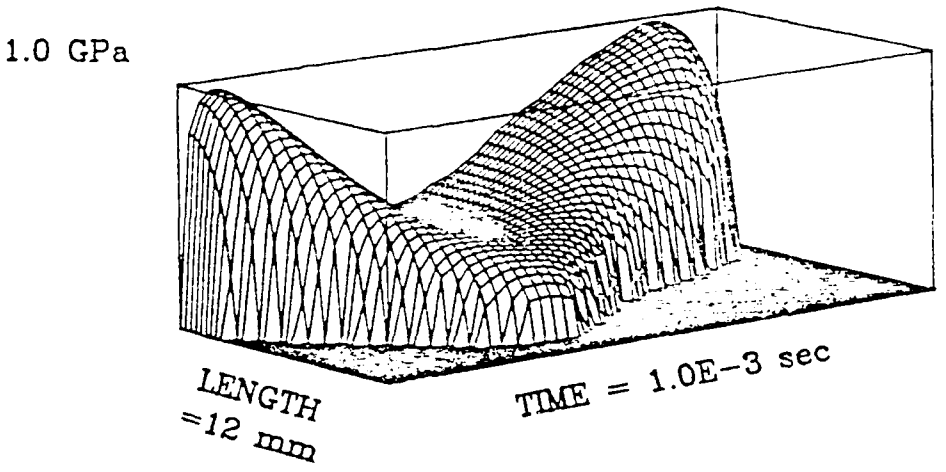

Fig. 6: Pressure Distribution for Simply Supported Plate (M = 1.5, V = 20 m/s)

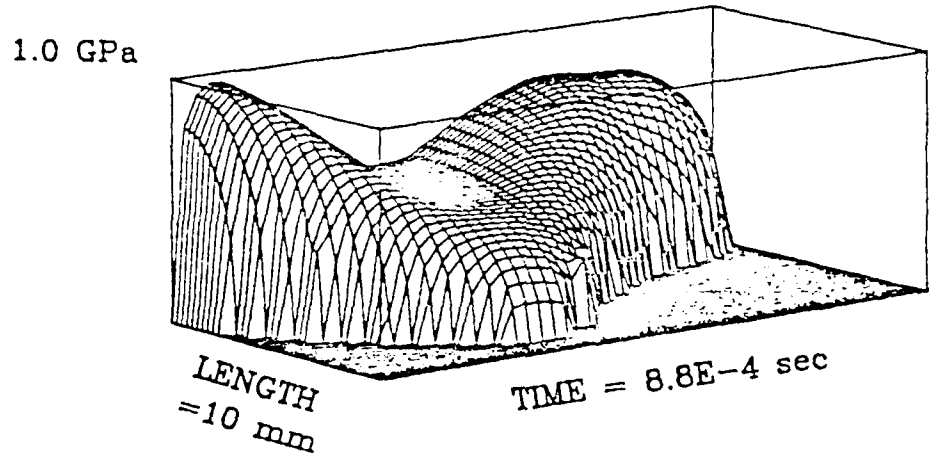

Fig. 7: Pressure Distribution for Simply Supported Plate (M = 2.0, V = 20 m/s)

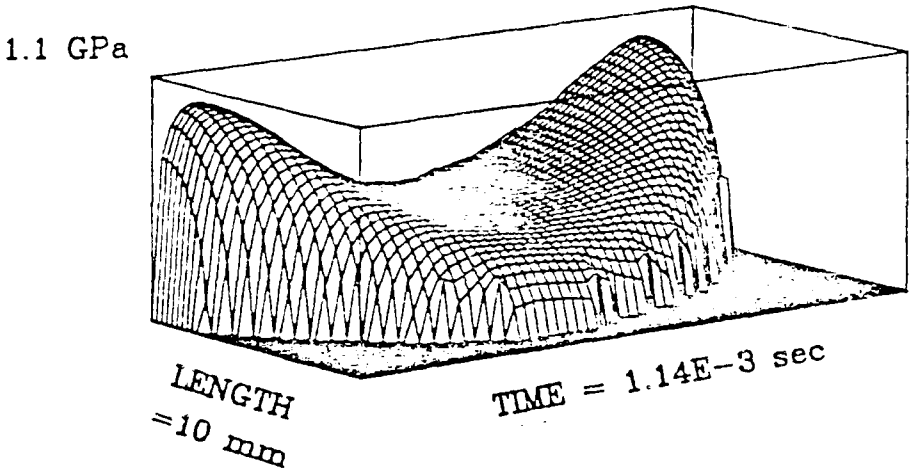

Fig. 8: Pressure Distribution for
Simply Supported Plate
(M = 1.0, V = 15 m/s)

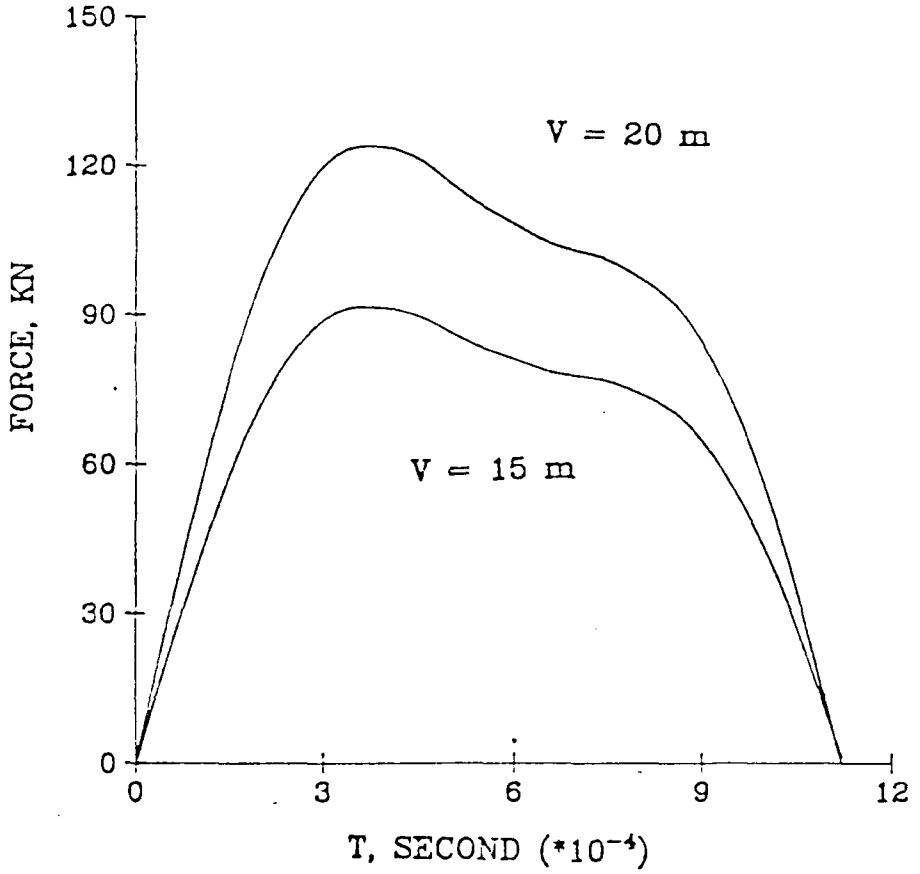

Fig. 9(a): Force History for Simply Supported Plate Subjected to Impact (M = 1.0)

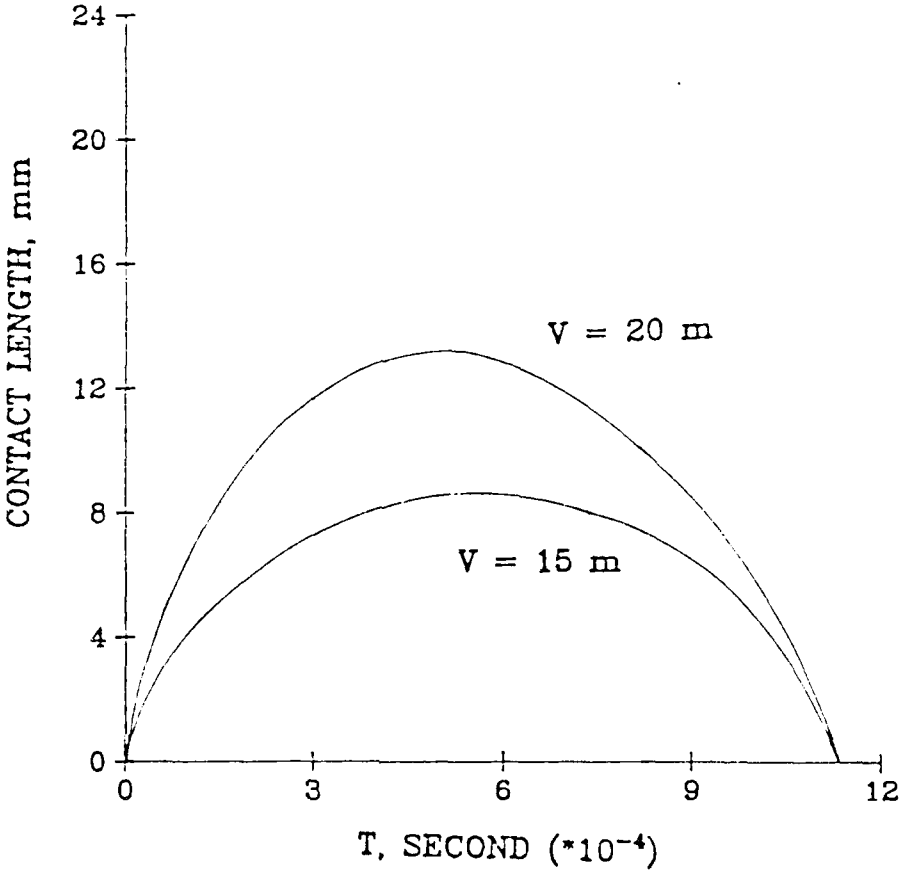

Fig. 9(b): Contact Length vs Time for Simply Supported Plate Subjected to Impact (V = 1.0)

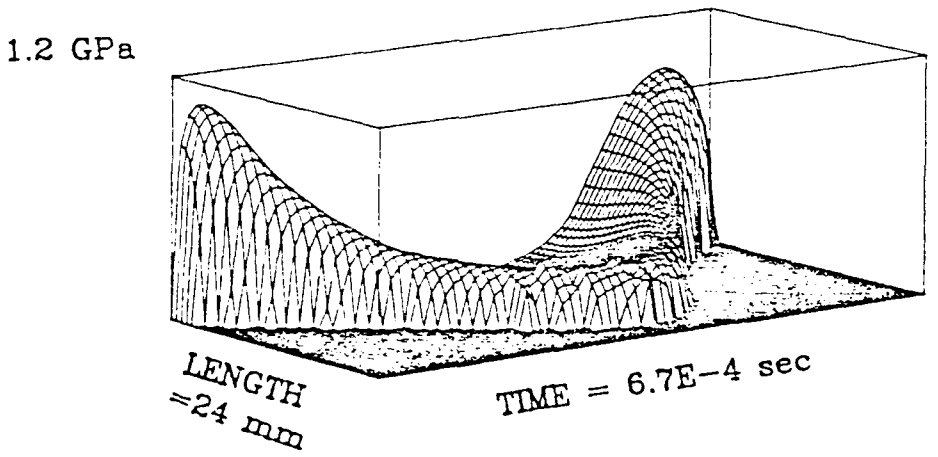

Fig. 10: Pressure Distribution for Clamped Plate
(V = 20 m/s, M = 1.0)

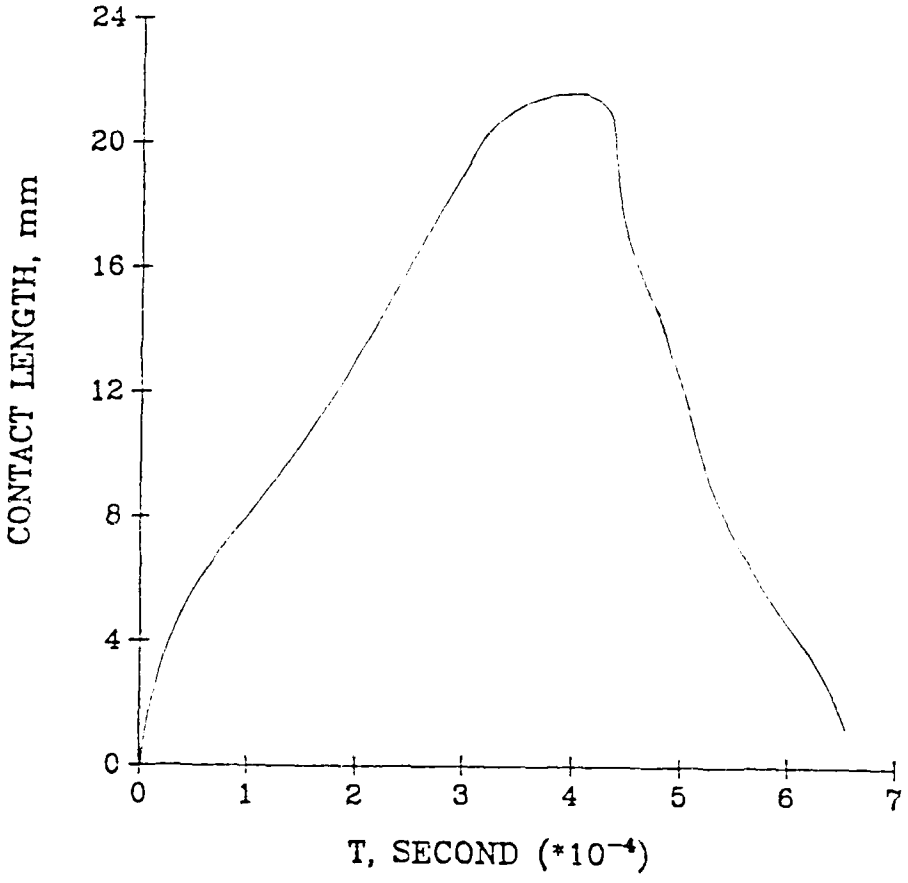

Fig. 11(a): Contact Length vs Time for Clamped Plate Subjected to Transverse Impact (V = 20 m/s, M = 1.0)

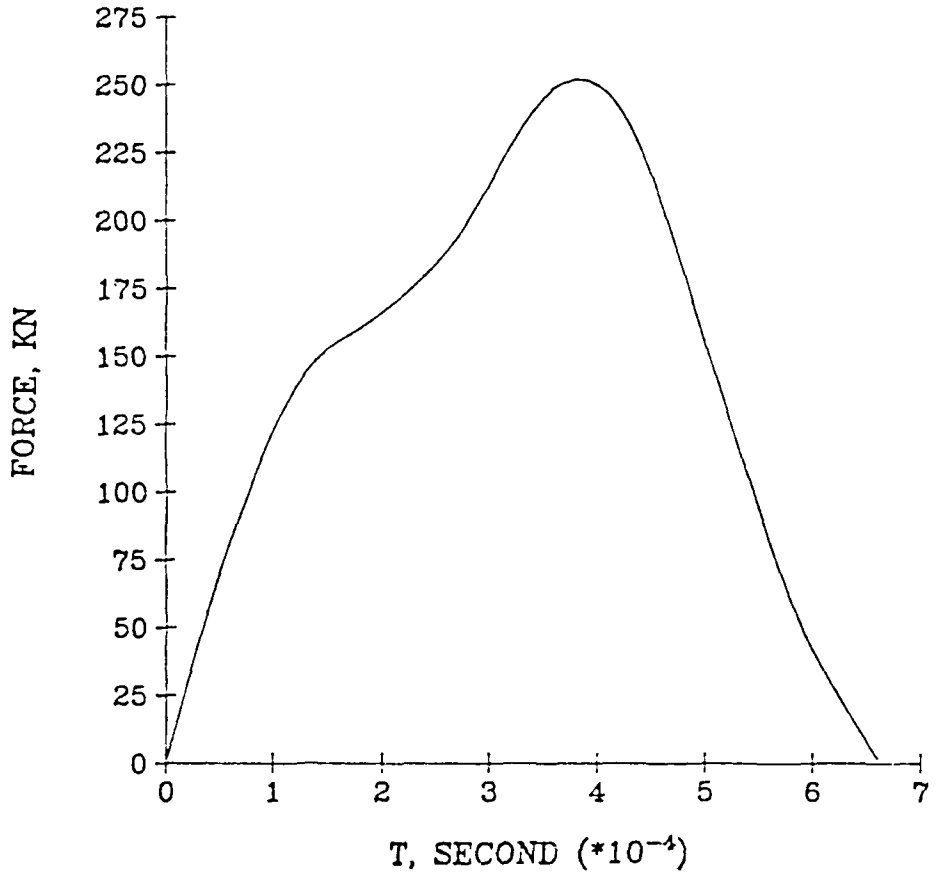

Fig. 11(b): Force History for Clamped Plate Subjected to Transverse Impact (V = 20 m/s, M = 1.0)

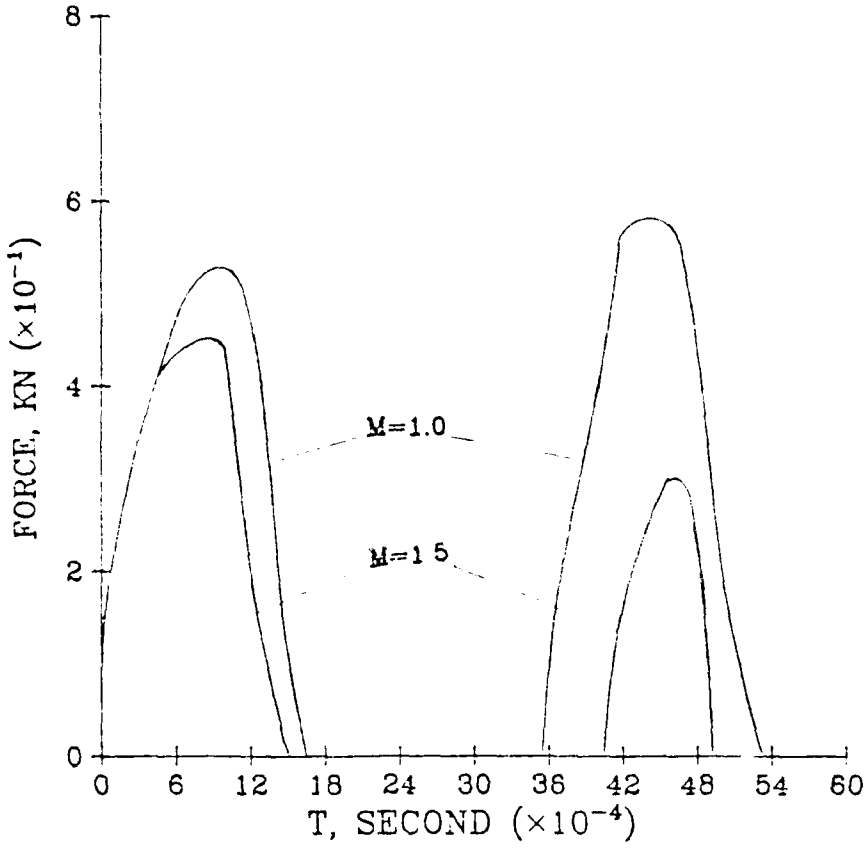

Fig. 12(a): Force History for Simply Supported Plate Subjected to Impact (V_0 = 2 m/s. Thickness of Plate = 0.125 cm)

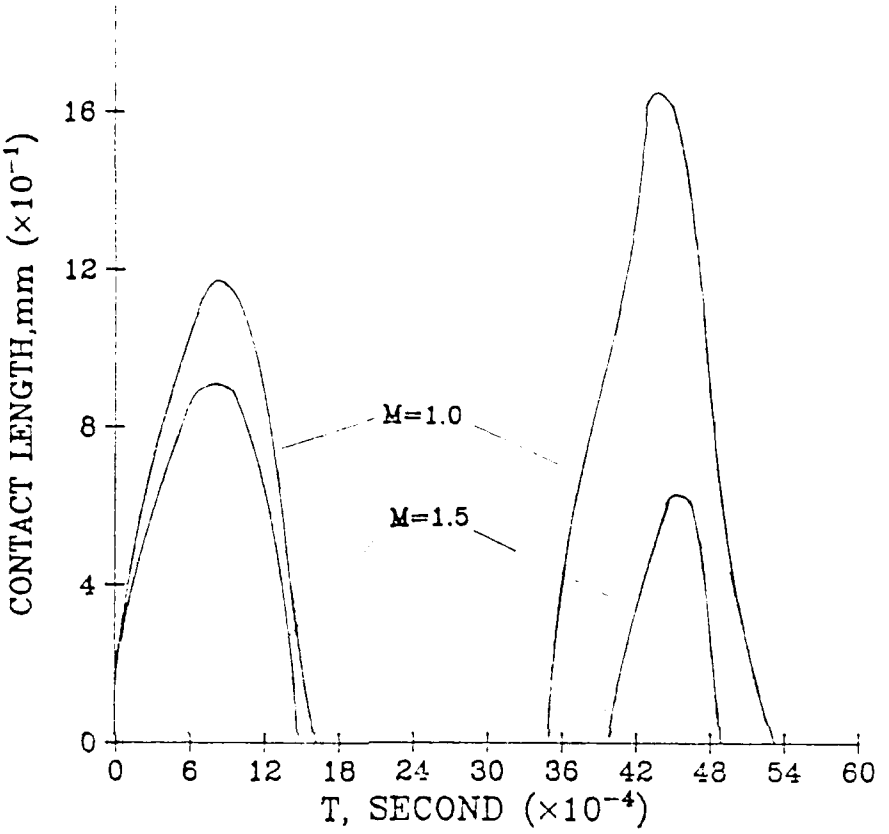

Fig. 11(b): Contact Length vs. Time for Simply Supported Plate Subject to Impact (V = 2 m/s, Thickness of Plate = 0.125 cm)

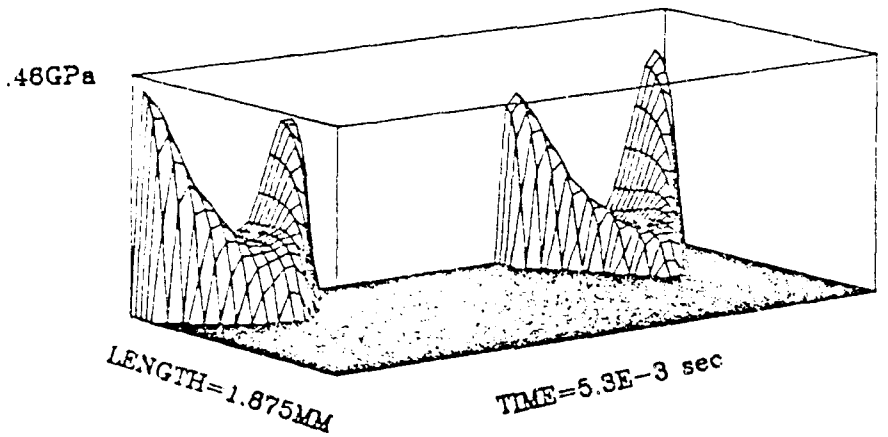

Fig. 13: Pressure Distribution for
Simply Supported Plate
($V^* = 1.0$, $V = 2$ m/s
Thickness of Plate
= 0.125 cm)

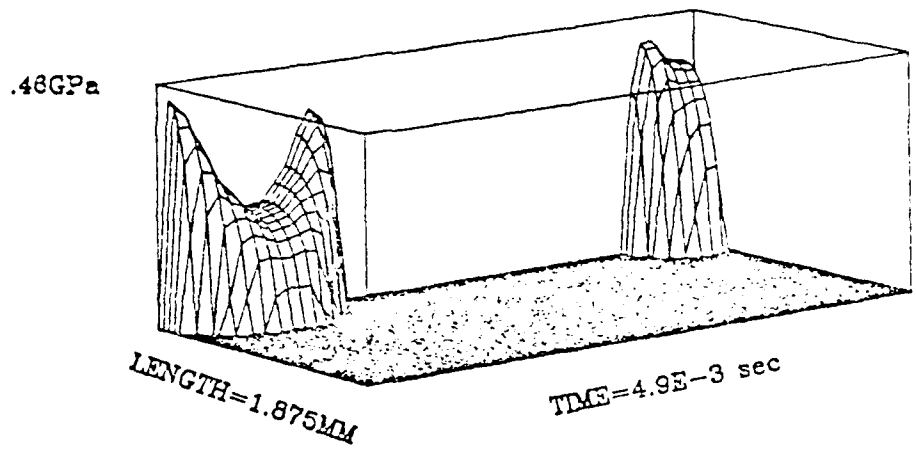

Fig. 14: Pressure Distribution for Simply Supported Plate (M = 1.5, V = 2 m/s. Thickness of Plate = 0.125 cm)

END

DTIC

7-86